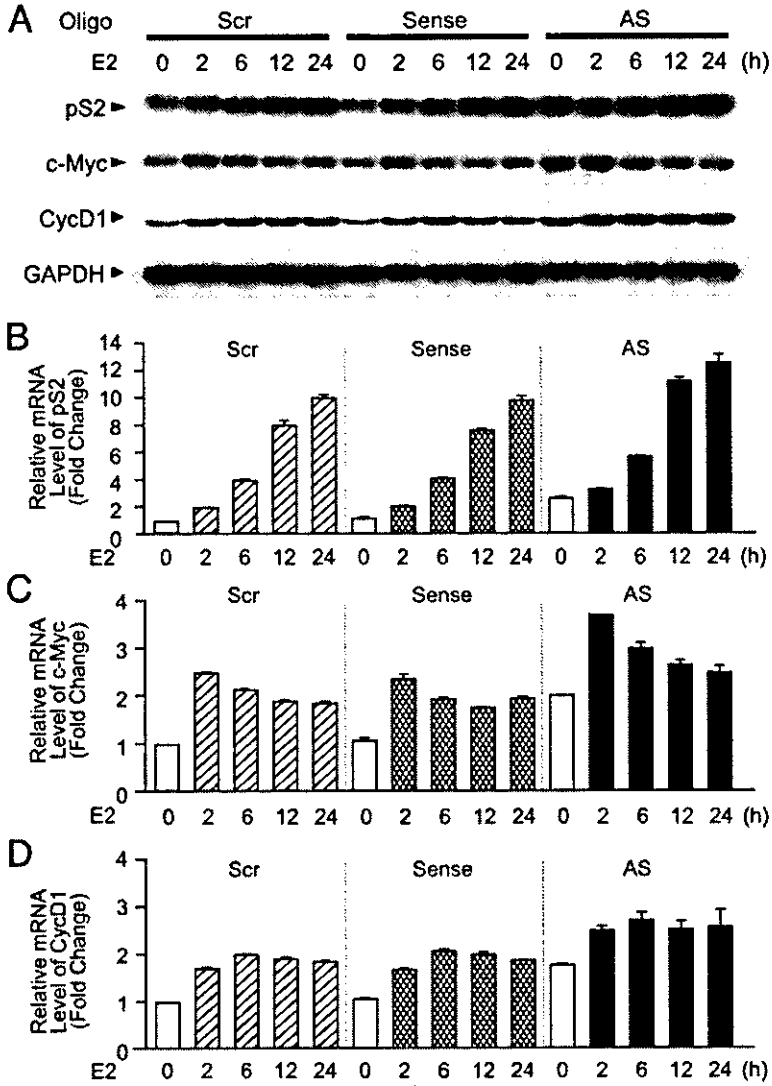

Fig. 8. PP5 AS Oligonucleotide Enhances E_2-Induced Transcription of Estrogen-Responsive Genes in MCF7 Cells

MCF7 cells were plated at a density of 1×10^6 cells per well on 10-cm plates and transfected with 5 μg control mismatch Scr, PP5 sense (Sense), or PP5 AS oligonucleotides for 12 h. Cells were serum starved for 24 h after the transfection and treated with E_2 (10 nM) for indicated times. Northern blot analysis was performed as indicated in Fig. 7. A, The representative result of three independent experiments of Northern blotting. B, C, and D, Quantification of mRNA levels of estrogen-responsive genes including pS2 (B), c-*myc* (C), and CycD1 (D) after normalization to GAPDH mRNA levels in MCF7 cells after E_2 treatment. Data are expressed as the mean ± SD values of fold change over control from three independent experiments. Data for cells transfected with Scr oligonucleotide and harvested at the starting point of E_2 treatments are used as control mRNA levels.

binding to ERα and ERβ. The TPR domains of PP5 may also function as an autoinhibitory region against phosphatase activity as removal of the domain produces a marked increase in activity (31). In contrast, PP2A acts in a form of heterotrimer like other members of the PPP family, except PP5, and it has been reported that the catalytic subunit of the phosphatase is required for the interaction with ERα. In regard to interacting functional domains of ERs, we have found E domains not containing an AD core region within AF-2 bind to PP5, whereas the A/B domain within AF-1 of ERα was reported to associate with PP2A. Thus it seems that ERs can be dephosphorylated by several kinds of protein phosphatases at different functional domains, leading to the more complex and subtle regulatory mechanisms for the receptors. Yet it is also noted that PP5 can exist in a native complex *in vivo* with the A subunit of PP2A via its TPR domains (20). It may be possible that PP5 directly interacts and cooperates with PP2A when the phosphatases bind to ERs and regulate the phosphorylation status of the receptors.

Notably, we showed that the truncated PP5 mutant consisting of only its TPR domains acts as a dominant negative PP5 because it increased the levels of ERα phosphorylation on S118 and transcriptional activation by ERα and ERβ. Our data suggest a physiological

role for PP5 in ER signaling *in vivo*. It has been shown that the TPR domains of PP5 also have dominant negative effects on glucocorticoid receptor (GR)-mediated transactivation (16). PP5 could regulate the phosphorylation state of steroid receptors or associated phosphoproteins. We speculate that the TPR domains of PP5 may form complexes with endogenous PP5, leading to inhibition of phosphatase activity of endogenous PP5. Another possibility is that the TPR domains of PP5 displace other interacting proteins of steroid receptors, which are crucial for the regulation of the receptors. Indeed, some of the TPR-containing proteins appear to compete with each other for binding to heat shock protein 90, a major molecular chaperone that forms heterocomplexes with steroid receptors and participates in the signaling pathways of the receptors including glucocorticoid receptor (GR) and ER (32, 33).

To confirm endogenous PP5 activity toward ERα function, we used an AS strategy to decrease PP5 expression in MCF7 cells. The phosphorothioate AS oligonucleotide was designed to target the region overlapping the translation start site. Treatment with PP5 AS oligonucleotide, but not with control Scr or PP5 sense oligonucleotides, led to a significant reduction of PP5 expression (Fig. 6C) and a proportional increase in S118 phosphorylation of ERα (Fig. 5, C and D), transcriptional activity by ERα (Fig. 6C), and expression of estrogen-targeted gene mRNAs (Fig. 8, A–D) in MCF cells. In a report using PP5 AS oligonucleotide targeting the 3′-untranslated region of PP5 for MCF7 cells, Urban *et al.* (34) concluded that treatment with up to 500 nM of PP5 AS had no apparent effect on estrogen-induced expression of c-*myc* and cyclin D1 mRNA. In contrast to their Northern blot result, we investigated the time-dependent mRNA expression of estrogen-targeted genes and confirmed that PP5 AS oligonucleotide at a concentration less than 70 nM significantly suppressed E_2-dependent mRNA expression of pS2, c-*myc*, and cyclin D1. Thus, we consider that PP5 is a critical regulator of ER function that could modulate phosphorylation states and transcriptional activities of the receptors.

On the basis of its interactions with other proteins and of studies in which PP5 activity was inhibited using recombinant DNA approaches and antisense oligonucleotide treatment, potential biological roles of PP5 have begun to be elucidated. PP5 has been shown to modulate GR signaling (16, 35), to promote cell growth (34, 36), and to terminate responses to oxidative stress (17). In regard to oxidative stress, PP5 is a physiological inhibitor of apoptosis signal-regulating kinase 1-c-Jun N-terminal kinase/p38 pathway, which plays a pivotal role in stress-induced apoptosis (17). PP5 also interacts with the anaphase-promoting complex and preserves the dephosphorylated or inactivated state of the complex before the activation occurs (19). The growth-promoting effect of PP5 on cell proliferation appears to be exerted by inhibiting both glucocorticoid- and p53-mediated signaling pathways leading to $p21^{WAF1/Cip1}$-mediated growth arrest (35, 36). Constitutive overexpression of PP5 in MCF7 cells converted the E_2-dependent phenotype of the cells into an E_2-independent one (34). Indeed, we also observed that adenoviral delivery of PP5 into MCF7 cells increases the number of proliferating cells by cell cycle analysis, as it decreases the percentage of cells at G_1 phase and accumulates the cells at S phase (data not shown). Although it seems paradoxical, we speculate that the proliferative function of overexpressed PP5 observed in MCF7 cells may result from a hyperactivity of the enzyme to inhibit growth-arresting factors including GR and p53, which overcomes PP5-mediated inhibition of ER function at physiological concentrations of the phosphatase.

In summary, we have demonstrated that PP5 directly binds to ERs and regulates ER phosphorylation and transcriptional activity in a negative manner. The inhibitory action of PP5 against ER phosphorylation and function may contribute to a regulatory system of ER-mediated signaling at physiological and pathophysiological status. Further study will be required to understand the distinct activity of PP5 in estrogen-dependent cell proliferation, which may be responsible for developing hormone-dependent tumors.

MATERIALS AND METHODS

Yeast Two-Hybrid Screening

To analyze the regulatory mechanism of ERs, we employed the yeast two-hybrid system to search for proteins that bind to ERs by using ERβ (1–481), a truncated human ERβ cDNA fragment containing 1–481 amino acids (24) as a bait. The bait plasmid was constructed in-frame with the LexA DNA-binding domain of the pEG202NLS plasmid (Origene Technologies Inc., Rockville, MD). A cDNA library derived from estrogen-depleted MCF7 cells in the pJG4–5 prey plasmid was screened for proteins that interact with ERβ (1–481) using the EGY48 yeast reporter strain and the pSH18–34 LacZ reporter plasmid. Plasmids of positive clones were recovered, and the cDNA inserts were sequenced. To examine the interaction between ERβ (1–481) and PP5, ERβ (1–481) and PP5 constructs were cotransformed along with the pSH18–34 reporter plasmid into the EGY48 yeast strain. Transcriptional activation of LacZ gene was examined in X-gal (5-bromo-4-chloro-3-indolyl-β-D-galactopyranoside)-containing medium. As PP5 cDNA was included in a galactose-inducible vector, pJG4–5, the interaction between ERβ (1–481) and PP5 was observed when the reporter yeast was transformed with a ERβ (1–481) construct pEG202NLS-ERβ (1–481) and cultured in galactose-containing medium.

GST Pull-Down Assay

GST constructs for full-length PP5 (GST-PP5) and truncated PP5 mutants GST-PP5 (2–71), GST-PP5 (28–165), GST-PP5 (2–181), GST-PP5 (2–132), and GST-PP5 (181–499), were prepared in pGEX4T-1 (Amersham Biosciences, Inc., Piscataway, NJ). With regard to structure of the truncated PP5 mutants, GST-PP5 (2–71) includes only one TPR domain. GST-PP5 (28–165) and GST-PP5 (2–181) contain four TPR

domains. GST-PP5 (2–312) consists of four TPR domains plus the N-terminal region of catalytic domain. GST-PP5 (181–499) includes the whole catalytic domain but not TPR domains. GST fusion proteins were induced, solubilized in solution A (20 mM Tris-HCl, pH 7.9; 10% glycerol; 80 mM KCl; 1 mM $MgCl_2$; 0.2 mM EDTA; 0.5 mM dithiothreitol; 0.5 mM phenylmethylsulfonyl fluoride; and 1% Triton X-100), and bound to glutathione-Sepharose 4B beads following the manufacturer's instruction (Amersham Biosciences, Inc.). GST fusion proteins bound to glutathione beads were incubated at 4 C for 1.5 h with ^{35}S-labeled ERα or ERβ, which was synthesized *in vitro* using the TnT-coupled reticulocyte lysate system (Promega Corp., Madison, WI). After the incubation, the beads were washed three times with solution A, and the complexes were separated by SDS-PAGE. The results were visualized using a Fuji FLA 3000 phosphoimaging analyzer (Fuji Film, Tokyo, Japan).

Mammalian Two-Hybrid Assay

The luciferase reporter plasmid TK-MH100 × 4Luc and the expression plasmids pCMX-GAL4 and pCMX-VP16 were kindly provided by K. Umesono (Kyoto University, Kyoto, Japan). pCMX-VP16-PP5 was constructed by an in-frame ligation of human PP5 cDNA to the VP16 transactivation domain in pCMX-VP16. pCMX-GAL4 constructs were generated by in-frame ligations of various ERα and ERβ cDNA fragments to the GAL4 DNA binding domain in pCMX-GAL4. The receptor domains encoded by ERα and ERβ cDNA fragments were as follows: for ERα, ABCD (amino acids 1–302), ABC (amino acids 1–263), E (amino acids 302–530), and a part of EF (amino acids 530–595) domains; for ERβ, ABCD (amino acids 1–248), ABC (amino acids 1–213), E (amino acids 248–481), and a part of EF (amino acids 481–530) domains. 293T cells were plated at a density of 6×10^4 cells per well of 24-well plates and incubated overnight. Cells were then cotransfected with plasmids containing 0.8 μg TK-MH100 × 4Luc, 0.7 μg pRL-TK vector (Promega), 0.2 μg VP16-PP5, and 0.1 μg GAL4 fusion constructs of ERα or ERβ using FuGENE 6 transfection reagent (Roche Diagnostics, Indianapolis, IN). Cells were cultured for 24 h and luciferase assays were performed using a Dual-Luciferase Assay System (Promega). Data are expressed as the mean ± SD of three independent experiments performed in triplicate.

Coimmunoprecipitation Assay

The GFP-tagged ERα construct was generated by an in-frame ligation of human ERα cDNA to downstream of GFP in pEGFP-C2 (BD Biosciences CLONTECH, Palo Alto, CA). The Flag-tagged pcDNA3 (Invitrogen, San Diego, CA) constructs pcDNA3-Flag-PP5 and pcDNA3-Flag-TPR were prepared by insertions of full-length PP5 and TPR domains (amino acids 28–165) into pcDNA3 containing Flag tag. 293T cells were plated at a density of 1×10^6 cells per dish in 10-cm dishes and cotransfected with 7.5 μg GFP-ERα and 7.5 μg Flag-PP5 or Flag-TPR by the calcium phosphate method. After 24 h, cells were incubated with PBS containing 5 mM hybrophobic lysine-specific cross-linker dithiobis[succinimidyl propionate] (Pierce Biotechnology, Inc., Rockford, IL) at 4 C for 30 min. The reaction was stopped by addition of 100 mM Tris-HCl, pH 7.5, at room temperature for 10 min. Cells were washed with PBS and lysed in immunoprecipitation buffer (50 mM Tris-HCl, pH 7.5, 150 mM NaCl, 1% Nonidet P-40, 0.5 mM aprotinin, 0.5 mM phenylmethylsulfonylfluoride). Lysates were cleared by centrifugation, and protein concentrations were determined by the Bradford method (Bio-Rad Laboratories, Inc., Hercules, CA). For immunoprecipitation, 1 mg of lysates were incubated with 10 μg of anti-Flag antibody M2 (Sigma Chemical Co., St. Louis, MO) for 3 h at 4 C, and then incubated with 20 μl of protein G-Sepharose beads (50% vol/vol slurry) (Amersham Biosciences, Inc.) for 90 min at 4 C. The beads were washed three times with immunoprecipitation buffer and resuspended in 20 μl of sample buffer for SDS-PAGE. Eluted proteins were subjected to SDS-PAGE, followed by electroblotting onto polyvinylidene difluoride membrane, and probed with antibodies against GFP (Medical & Biological Laboratories Co., Ltd., Nagoya, Japan). The antibody-antigen complexes were detected using the enhanced chemiluminescence system (Amersham Biosciences, Inc.) according to the manufacturer's instruction. In experiments for examining the interaction between endogenous PP5 and ERα, the extracts from MCF7 cells were immunoprecipitated with an anti-PP5 antibody PP5/PPT (BD Biosciences, San Jose, CA) or nonimmune serum and probed by an anti-ERα antibody H-184 (Santa Cruz Biotechnology, Santa Cruz, CA).

Adenoviral Gene Expression

Adenoviral constructs of Flag-tagged human PP5 (Ad-PP5) and GFP-fusion histone H2B (Ad-GFP) were prepared in an adenovirus vector using Adenovirus Expression Vector Kit (Takara Bio Inc., Shiga, Japan) (37, 38). MCF7 cells were infected with the recombinant adenoviruses at a multiplicity of infection (MOI) of 10 for 12 h. The infected cells were serum starved for 24 h in phenol red-free DMEM and treated with 10 nM E_2 in DMEM containing 10% dextran-coated charcoal-treated fetal calf serum (dccFCS) for the indicated times.

Oligonucleotide Treatment

Twenty-three-base phosphorothioate oligonucleotides were prepared by Invitrogen. Sequences for PP5 AS, PP5 sense, and control Scr oligonucleotides were 5′-CTCTCGCCCTC-CGCCATCGCCAT-3′, 5′-ATGGCGATGGCGGAGGGCGAGAG-3′, and 5′-GCAGTGGCGAGCTGAGAGAGGGG-3′, respectively. MCF7 cells were incubated with phenol red-free DMEM containing 10% dccFCS before experiments. Cells were transfected with oligonucleotides using GeneSilencer reagent (GeneTherapy Systems, Inc., San Diego, CA) according to the procedure recommended by the manufacturer. Twelve hours after transfection, cells were fed with serum-starved DMEM, or phenol red-free DMEM containing 10% dccFCS supplemented with or without E_2. Cells were used for experiments involving ER phosphorylation, transactivation, and expression of estrogen target genes.

Transcription Assay of ER

Expression vectors of S118A (HE457) and S118E (HE458) mutants of ERα were the gifts from Dr. P. Chambon (3). N-terminal Flag-tagged pcDNA3 constructs including full-length PP5, TPR domains, and catalytic domain were generated. 293T cells at a density of 1×10^4 cells per well on 24-well plates were transfected with 0.8 μg ERE-tk-Luc, 0.7 μg pRL-CMV (Promega), 5 ng of expression vectors for full-length ERα/ERβ or ERα mutants, and 0–50 ng of expression vectors for full-length or truncated PP5 in phenol red-free DMEM containing 10% dccFCS using FuGENE 6 transfection reagent (Roche Diagnostics). Twelve hours after transfection, cells were treated with or without 10 nM E_2 for 24 h and luciferase assays were performed. Data were represented as the mean ± SD of three independent experiments performed in triplicate.

Northern Blot Analysis and Probes

The cDNAs encoding full-length human pS2, human c-*myc*, human cyclin D1, and human GAPDH were cloned by RT-PCR and verified by sequencing. Probes for Northern blot analysis were prepared by labeling the cloned cDNAs with [α-^{32}P]dCTP using the Random Primer Labeling Kit (Takara

Bio Inc.). Total RNAs (20 μg) were separated in 1% formaldehyde denaturing agarose gels and transferred to Hybond-NX membranes (Amersham Biosciences, Inc.). Blotted membranes were hybridized with the ^{32}P-labeled probes in a hybridization buffer (0.1% sodium dodecyl sulfate (SDS), 50% formamide, 5× sodium saline citrate (SSC), 50 mM $NaPO_4$ (pH 6.8), 0.1% sodium pyrophosphate, 5 × Denhardt's solution, and 50 μg/ml salmon sperm DNA] at 42 C overnight. Membranes were then washed with 2× SSC, 0.1% SDS at 42 C for 30 min and 0.2× SSC, 0.1% SDS at 42 C for 30 min. Radioactivities of the signals were quantified using a Fuji FLA 3000 phosphoimaging analyzer (Fuji Photo Film, Tokyo, Japan). The mRNA levels for estrogen-targeted genes at each time point were determined by the signal intensities normalized by that of GAPDH mRNA level in an identical sample. Data for cells treated with vehicle and harvested at the starting point of E_2 treatments are used as control mRNA levels. Data are expressed as the mean ± SD values of fold change over control from three independent experiments.

Analysis for Phosphorylation State of ERα at S118

MCF7 cells were plated at a density of 1.4 × 10^5 cells on six-well plates and transfected with 1 μg of expression plasmids for full-length PP5, TPR domains, or an empty vector for 12 h using FuGENE 6 transfection reagent (Roche Diagnostics). In experiments using oligonucleotides, cells were transfected with PP5 sense, AS, or control mismatch Scr oligonucleotides for 12 h using GeneSilencer reagent. In a preliminary experiment, we confirmed that the transfection efficiency of pEGFP-C1 vector (BD Biosciences CLONTECH) into MCF7 cells was 32% using FuGENE 6 transfection reagent. Transfected cells were serum starved for 24 h and treated with E_2 (10 nM), EGF(100 ng/ml), or vehicles. Cell extracts were subjected to immunoblotting using a specific antibody against phosphorylated ERα at S118 (16J4)(Cell Signaling Technology, Beverly, MA). Quantification of signal intensities was performed using LAS 1000 image analyzer (Fuji Photo Film). Three independent experiments were performed, and phosphorylation levels at ERα S118 were normalized by total protein amounts of ERα.

Cell Cycle Analysis

For flow cytometry analysis, MCF7 cells were transduced with recombinant adenoviruses Ad-PP5 or Ad-GFP. Twelve hours after infection, cells were cultured in serum-deleted medium for 24 h and treated with E_2 (10 nM). Cells were trypsinized, fixed with 70% ethanol, treated with RNase A (100 μg/ml), and then stained with propidium iodide (10 μg/ml). Cells were analyzed by FACS Calibur flow cytometer (Becton Dickinson and Co., Mountain View, CA) and the cell-cycle profile was determined using ModFit LT software (Becton Dickinson).

Acknowledgments

We thank Dr. P. Chambon for kindly providing HE457 and HE458 plasmids, and T. Hishinuma, T. Ichikawa, and A. Harashima for their technical assistance.

Received August 9, 2003. Accepted January 27, 2004.

Address all correspondence and requests for reprints to: Satoshi Inoue, Division of Gene Regulation and Signal Transduction, Research Center for Genomic Medicine, Saitama Medical School, 1397-1 Yamane, Hidaka-shi, Saitama 350-1241, Japan. E-mail: INOUE-GER@h.u-tokyo.ac.jp.

This work was supported in part by grants-in-aid from the Ministry of Health, Labor and Welfare; from the Ministry of Education, Culture, Sports, Science and Technology of Japan; from Kanzawa Medical Research Foundation; and from Novartis Foundation (Japan) for the Promotion of Science.

REFERENCES

1. Muramatsu M, Inoue S 2000 Estrogen receptors: how do they control reproductive and nonreproductive functions? Biochem Biophys Res Commun 270:1–10
2. Shao D, Lazar MA 1999 Modulating nuclear receptor function: may the phos be with you. J Clin Invest 103: 1617–1618
3. Ali S, Metzger D, Bornert JM, Chambon P 1993 Modulation of transcriptional activation by ligand-dependent phosphorylation of the human oestrogen receptor A/B region. EMBO J 12:1153–1160
4. Kato S, Endoh H, Masuhiro Y, Kitamoto T, Uchiyama S, Sasaki H, Masushige S, Gotoh Y, Nishida E, Kawashima H, Metzger D, Chambon P 1995 Activation of the estrogen receptor through phosphorylation by mitogen-activated protein kinase. Science 270:1491–1494
5. Tremblay A, Tremblay GB, Labrie F, Giguere V 1999 Ligand-independent recruitment of SRC-1 to estrogen receptor β through phosphorylation of activation function AF-1. Mol Cell 3:513–519
6. Chen D, Pace PE, Coombes RC, Ali S 1999 Phosphorylation of human estrogen receptor α by protein kinase A regulates dimerization. Mol Cell Biol 19:1002–1015
7. Chen D, Riedl T, Washbrook E, Pace PE, Coombes RC, Egly JM, Ali S 2000 Activation of estrogen receptor α by S118 phosphorylation involves a ligand-dependent interaction with TFIIH and participation of CDK7. Mol Cell 6:127–137
8. Le Goff P, Montano MM, Schodin DJ, Katzenellenbogen BS 1994 Phosphorylation of the human estrogen receptor. Identification of hormone-regulated sites and examination of their influence on transcriptional activity. J Biol Chem 269:4458–4466
9. Joel PB, Traish AM, Lannigan DA 1998 Estradiol-induced phosphorylation of serine 118 in the estrogen receptor is independent of p42/p44 mitogen-activated protein kinase. J Biol Chem 273:13317–13323
10. Barford D, Das AK, Egloff MP 1998 The structure and mechanism of protein phosphatases: insights into catalysis and regulation. Annu Rev Biophys Biomol Struct 27:133–164
11. Cohen PT 1997 Novel protein serine/threonine phosphatases: variety is the spice of life. Trends Biochem Sci 22:245–251
12. Chen MX, McPartlin AE, Brown L, Chen YH, Barker HM, Cohen PT 1994 A novel human protein serine/threonine phosphatase, which possesses four tetratricopeptide repeat motifs and localizes to the nucleus. EMBO J 13: 4278–4290
13. Hirano T, Kinoshita N, Morikawa K, Yanagida M 1990 Snap helix with knob and hole: essential repeats in *S. pombe* nuclear protein nuc2+. Cell 60:319–328
14. Sikorski RS, Boguski MS, Goebl M, Hieter P 1990 A repeating amino acid motif in CDC23 defines a family of proteins and a new relationship among genes required for mitosis and RNA synthesis. Cell 60:307–317
15. Blatch GL, Lassle M 1999 The tetratricopeptide repeat: a structural motif mediating protein-protein interactions. Bioessays 21:932–939
16. Chen MS, Silverstein AM, Pratt WB, Chinkers M 1996 The tetratricopeptide repeat domain of protein phosphatase 5 mediates binding to glucocorticoid receptor heterocomplexes and acts as a dominant negative mutant. J Biol Chem 271:32315–32320
17. Morita K, Saitoh M, Tobiume K, Matsuura H, Enomoto S, Nishitoh H, Ichijo H 2001 Negative feedback regulation of

ASK1 by protein phosphatase 5 (PP5) in response to oxidative stress. EMBO J 20:6028–6036
18. Chinkers M 1994 Targeting of a distinctive protein-serine phosphatase to the protein kinase-like domain of the atrial natriuretic peptide receptor. Proc Natl Acad Sci USA 91:11075–11079
19. Ollendorff V, Donoghue DJ 1997 The serine/threonine phosphatase PP5 interacts with CDC16 and CDC27, two tetratricopeptide repeat-containing subunits of the anaphase-promoting complex. J Biol Chem 272:32011–32018
20. Lubert EJ, Hong Y, Sarge KD 2001 Interaction between protein phosphatase 5 and the A subunit of protein phosphatase 2A: evidence for a heterotrimeric form of protein phosphatase 5. J Biol Chem 276:38582–38587
21. Brzozowski AM, Pike AC, Dauter Z, Hubbard RE, Bonn T, Engstrom O, Ohman L, Greene GL, Gustafsson JA, Carlquist M 1997 Molecular basis of agonism and antagonism in the oestrogen receptor. Nature 389:753–758
22. Shiau AK, Barstad D, Loria PM, Cheng L, Kushner PJ, Agard DA, Greene GL 1998 The structural basis of estrogen receptor/coactivator recognition and the antagonism of this interaction by tamoxifen. Cell 95:927–937
23. Pike AC, Brzozowski AM, Hubbard RE, Bonn T, Thorsell AG, Engstrom O, Ljunggren J, Gustafsson JA, Carlquist M 1999 Structure of the ligand-binding domain of oestrogen receptor β in the presence of a partial agonist and a full antagonist. EMBO J 18:4608–4618
24. Ogawa S, Inoue S, Orimo A, Hosoi T, Ouchi Y, Muramatsu M 1998 Cross-inhibition of both estrogen receptor α and β pathways by each dominant negative mutant. FEBS Lett 423:129–132
25. Brown AM, Jeltsch JM, Roberts M, Chambon P 1984 Activation of pS2 gene transcription is a primary response to estrogen in the human breast cancer cell line MCF-7. Proc Natl Acad Sci USA 81:6344–6348
26. Dubik D, Shiu RP 1992 Mechanism of estrogen activation of c-myc oncogene expression. Oncogene 7:1587–1594
27. Sabbah M, Courilleau D, Mester J, Redeuilh G 1999 Estrogen induction of the cyclin D1 promoter: involvement of a cAMP response-like element. Proc Natl Acad Sci USA 96:11217–11222
28. Castro-Rivera E, Samudio I, Safe S 2001 Estrogen regulation of cyclin D1 gene expression in ZR-75 breast cancer cells involves multiple enhancer elements. J Biol Chem 276:30853–30861
29. Smith CL 1998 Cross-talk between peptide growth factor and estrogen receptor signaling pathways. Biol Reprod 58:627–632
30. Lu Q, Surks HK, Ebling H, Baur WE, Brown D, Pallas DC, Karas RH 2003 Regulation of estrogen receptor α-mediated transcription by a direct interaction with protein phosphatase 2A. J Biol Chem 278:4639–4645
31. Sinclair C, Borchers C, Parker C, Tomer K, Charbonneau H, Rossie S 1999 The tetratricopeptide repeat domain and a C-terminal region control the activity of Ser/Thr protein phosphatase 5. J Biol Chem 274:23666–23672
32. Owens-Grillo JK, Hoffmann K, Hutchison KA, Yem AW, Deibel Jr MR, Handschumacher RE, Pratt WB 1995 The cyclosporin A-binding immunophilin CyP-40 and the FK506-binding immunophilin hsp56 bind to a common site on hsp90 and exist in independent cytosolic heterocomplexes with the untransformed glucocorticoid receptor. J Biol Chem 270:20479–20484
33. Ratajczak T, Carrello A 1996 Cyclophilin 40 (CyP-40), mapping of its hsp90 binding domain and evidence that FKBP52 competes with CyP-40 for hsp90 binding. J Biol Chem 271:2961–2965
34. Urban G, Golden T, Aragon IV, Scammell JG, Dean NM, Honkanen RE 2001 Identification of an estrogen-inducible phosphatase (PP5) that converts MCF-7 human breast carcinoma cells into an estrogen-independent phenotype when expressed constitutively. J Biol Chem 276:27638–27646
35. Zuo Z, Urban G, Scammell JG, Dean NM, McLean TK, Aragon I, Honkanen RE 1999 Ser/Thr protein phosphatase type 5 (PP5) is a negative regulator of glucocorticoid receptor-mediated growth arrest. Biochemistry 38: 8849–8857
36. Zuo Z, Dean NM, Honkanen RE 1998 Serine/threonine protein phosphatase type 5 acts upstream of p53 to regulate the induction of p21(WAF1/Cip1) and mediate growth arrest. J Biol Chem 273:12250–12258
37. Niwa H, Yamamura K, Miyazaki J 1991 Efficient selection for high-expression transfectants with a novel eukaryotic vector. Gene 108:193–199
38. Miyake S, Makimura M, Kanegae Y, Harada S, Sato Y, Takamori K, Tokuda C, Saito I 1996 Efficient generation of recombinant adenoviruses using adenovirus DNA-terminal protein complex and a cosmid bearing the full-length virus genome. Proc Natl Acad Sci USA 93:1320–1324

Molecular Endocrinology **is published monthly by The Endocrine Society (http://www.endo-society.org), the foremost professional society serving the endocrine community.**

Available online at www.sciencedirect.com
SCIENCE DIRECT®
Biochemical and Biophysical Research Communications 325 (2004) 1312–1317
BBRC
www.elsevier.com/locate/ybbrc

Identification and functional analysis of consensus androgen response elements in human prostate cancer cells☆

Kuniko Horie-Inoue[a], Hidemasa Bono[b], Yasushi Okazaki[b], Satoshi Inoue[a,c,*]

[a] *Division of Gene Regulation and Signal Transduction, Research Center for Genomic Medicine, Saitama Medical School, 1397-1 Yamane, Hidaka-shi, Saitama 350-1241, Japan*
[b] *Division of Functional Genomics and Systems Medicine, Research Center for Genomic Medicine, Saitama Medical School, 1397-1 Yamane, Hidaka-shi, Saitama 350-1241, Japan*
[c] *Department of Geriatric Medicine, Faculty of Medicine, The University of Tokyo, 7-3-1 Hongo, Bunkyo-ku, Tokyo 113-8655, Japan*

Received 26 October 2004
Available online 11 November 2004

Abstract

Androgen receptor (AR) recognizes and binds to 15-bp palindromic androgen response element (ARE) sequences with high affinity in vitro, which consist of two hexameric half-sites arranged as inverted repeats with a 3-bp spacer. Although a few near-consensus ARE sequences have been actually identified in the transcriptional regulatory regions of androgen-responsive genes, it has been unclear whether the exact consensus sequences function as bona fide AREs in vivo. A genome-wide in silico screening of palindromic AREs identified 563 exact consensus sequences in the human genome. The distribution of perfect palindromic AREs among the chromosomes is basically consistent with the length of chromosomes. Using human prostate cancer cell line LNCaP treated with a synthetic androgen R1881 as a model, in vivo AR binding abilities of 21 consensus AREs were analyzed by chromatin immunoprecipitation. Of 21 genomic fragments containing perfect AREs in chromosome X, 8 fragments recruited more ARs (>4-fold enrichment) even compared with the proximal ARE region of prostate-specific antigen. A couple of proximal genes or putative transcripts in the vicinity of the perfect AREs were found to be androgen-responsive analyzed by quantitative RT-PCR. Our results suggest that some of perfect palindromic AREs could function as in vivo AR binding sites in the human genome and regulate gene transcription.

Keywords: Androgen receptor; Androgen response element; Androgen-responsive gene; Chromatin immunoprecipitation; Prostate cancer

The androgen receptor (AR), a member of nuclear receptor superfamily that functions as a ligand-dependent transcription factor, plays an essential role in male sexual differentiation as well as prostate development and carcinogenesis. Forming complexes with coactivators and general transcription factors, ligand-stimulated AR binds to *cis*-acting androgen response elements (AREs) in the regulatory regions of androgen-responsive genes and modulates the transcription of target genes. The palindromic 15-bp sequence, which consists of two hexameric half-sites (5′-AGAACA-3′) arranged as an inverted repeat with a 3-bp spacer, has been identified as the consensus sequence for AR binding [1,2]. Although near-consensus ARE sequences that match at least 9 of 12 nucleotides have been found in the regulatory regions of several androgen-responsive genes [1], none of the perfect consensus ARE has yet been identified. A question arises whether the palindromic ARE consensus sequence functions as a bona fide AR binding

☆ *Abbreviations:* AR, androgen receptor; ARE, androgen response element; BCOR, BCL-6 interacting corepressor; ChIP, chromatin immunoprecipitation; GAPDH, glyceraldehyde-3-phosphate dehydrogenase; PCYT1B, phosphorylcholine transferase B; PSA, prostate-specific antigen; RT-PCR, reverse transcription-polymerase chain reaction.

* Corresponding author. Fax: +81 3 5800 6530.
E-mail address: INOUE-GER@h.u-tokyo.ac.jp (S. Inoue).

0006-291X/$ - see front matter © 2004 Elsevier Inc. All rights reserved.
doi:10.1016/j.bbrc.2004.10.174

site that regulates transcription of proximal androgen-responsive genes in vivo.

In the present study, we identified perfect ARE sites in silico based on the human genome sequences that are available from public database and analyzed experimentally the functions of consensus AREs in terms of AR binding abilities in vivo and potential androgen-dependent transcription regulation of proximal genes. Focusing on the chromosome X, we actually identified several AR binding sites among the computationally identified perfect ARE sequences. A couple of proximal RNA transcripts in the vicinity of perfect AREs were androgen-responsive, suggesting that some of the consensus ARE sites have potentials to activate transcription of nearby genes. Our combined approach of characterization of ARE sites will contribute to the systematic elucidation of the gene regulatory network mediated by androgen, which will be pivotal for the development of prostate cancer.

Materials and methods

Bioinformatics. Consensus AREs in the human genome (Human 34d Gene Build retrieved from Ensembl ftp site [3]) were screened utilizing in-house Perl script and a program for regular expression search of a nucleotide sequence (program name: dreg) in EMBOSS package [4]. The regular expression pattern for ARE was obtained from a recent literature by Nelson et al. [1], in which the palindromic 5′-AGAACAnnnTGTTCT-3′ sequence corresponding to the ARE sequence in TRANSFAC database [5] was used as a consensus sequence.

Cell culture. Human prostate cancer LNCaP cells were purchased from American Type Culture Collection (Rockville, MD) and maintained in RPMI 1640 supplemented with 4.5 g/dl glucose, 1 mM sodium pyruvate, 10 mM Hepes, and 10% fetal bovine serum (FBS). Prior to hormone addition, cells were cultured for 2 days in phenol red-free RPMI 1640 supplemented with 5% dextran–charcoal stripped FBS (dcc-FBS) and one day in phenol red-free RPMI 1640 supplemented with 2.5% dcc-FBS.

Chromatin immunoprecipitation assay. LNCaP cells (8×10^7) after 72-h hormone depletion were treated with 10 nM of R1881 (NEN Life Science Products, Boston, MA) or 0.1% ethanol for 24 h. Cells were fixed in 1% formaldehyde for 5 min at room temperature. Chromatin was sheared to an average size of 500 bp by sonication using a Bioruptor ultrasonicator (Cosmo-Bio, Tokyo, Japan). Lysates corresponding to 2×10^7 cells were rotated at 4 °C for overnight with 3 μg of polyclonal anti-AR antibody (H-280, Santa Cruz Biotechnology, Santa Cruz, CA) or non-specific rabbit IgG (Sigma). Salmon sperm DNA/protein A–agarose (Upstate Biotechnology, Lake Placid, NY) was added and incubated for 2 h. Washing and reversal of cross-links was performed as described [6]. Precipitated DNA fragments were quantified by quantitative real-time PCR using the Applied Biosystems 7000 sequence detector (Foster City, CA) based on SYBR Green I

Table 1
Primers for quantitative ChIP assay and RT-PCR

Target	Forward primer sequence	Reverse primer sequence
ARE sites[a]		
X1	5′-GTGCTTTGCAGGCAGTGATG-3′	5′-TCATTCCTTTGTTTTACTGAGAGTTCA-3′
X2	5′-GCAACTGCAAAGCCAAAATG-3′	5′-ATCTGTTTCCCATCTCCGTATATGTA-3′
X3	5′-CCAAAAAGCCCCTAGGAAAGA-3′	5′-AACCAGCAGTGTTTGCTCCAA-3′
X4	5′-CCAGGGCTCCTCCTTTGG-3′	5′-ATCTGACCCTGTGCATTTGAGA-3′
X5	5′-ACAGGTGCAAACACACAAAAGC-3′	5′-ACCCTTTCCTGGTCCTTTGTC-3′
X6	5′-ACAACAAATTCACCTGAGGTTCATAT-3′	5′-GCTTATCCAGGGACATCAGGTT-3′
X7	5′-CCAAATATGTCCATTCATCCAACA-3′	5′-GGAAACATACGCATTGCCTAGAA-3′
X8	5′-TTAATGTCTCTGTGAACCATTCTTCTG-3′	5′-GGTAACTACTGGGAAGGGAATTAGC-3′
X9	5′-CTGAGGGCGGACCTTGTTAAG-3′	5′-GCTCCAGGAGCTCTACGAGGTT-3′
X10	5′-TTAACAAAAAGCCAAGAGTGACAA-3′	5′-ACATCTTTTTTTCTTTGCTCCAGAA-3′
X11	5′-GAAGGTCCGTTGAGTTTATCTATTC-3′	5′-GGAAGTTTTCAGACATTTCTTCAG-3′
X12	5′-TGTGTAAAACACTCAACAAGTTAGAACA-3′	5′-CCTTGCCTTCTTTCTGATCTTAGG-3′
X13	5′-CGGGCAGTGGAAAAGCAA-3′	5′-CCTGTGTCTCCTCAAAAGAAATGA-3′
X14	5′-CAGTTCTGATGTGGTAAGTGGAAGA-3′	5′-GGTGAGTGGCGAAGTGGTAAC-3′
X15	5′-TCCCAGTTTCTCAGGGATCACT-3′	5′-TCTCCCACATGAAACAACTAAAAAGT-3′
X16	5′-AGGGCCAGCTTTATTAAGAACAGA-3′	5′-CTGTAGGAGCCCTGCAAGGT-3′
X17	5′-AATGTTTGCTTACTGCAAGTGTACT-3′	5′-GTGTGGGTTGCATGTACTGC-3′
X18	5′-TTTTGTCCCAGTCCTACATCTTGTT-3′	5′-GCTCATGTCCTCTATAGCCCTACA-3′
X19	5′-GCAGATTTTAAACCACAGTATTAAGTCAAA-3′	5′-GAGGGTACAGAGGAGCCAAAGA-3′
X20	5′-CAGAATCTGTAGCCAAACTACGAACT-3′	5′-CAGCCTGGCCCTTTTACTGA-3′
X21	5′-TCCTAGGAGAAATGGCTGATTCC-3′	5′-CAAAGTGTCATTATTCAGTGTACAACTCTAC-3′
PSA proximal promoter	5′-TCTGCCTTTGTCCCCTAGAT-3′	5′-AACCTTCATTCCCCAGGACT-3′
PSA distal promoter	5′-ACAGACCTACTCTGGAGGAAC-3′	5′-AAGACAGCAACACCTTTTT-3′
PSA coding	5′-GCCCTGCCCGAAAGG-3′	5′-GATCCACTTCCGGTAATGCA-3′
GAPDH coding[b]	5′-GGTGGTCTCCTCTGACTTCAACA-3′	5′-GTGGTCGTTGAGGGCAATG-3′
PCYT1B coding	5′-GCAGGGATGTTCGTTCCAA-3′	5′-CTGGTAATGATGTCCGATGTTGA-3′
NM_144657 coding	5′-CAGCAACAACAGGAACCTCTTTG-3′	5′-CGAGCAATATTAACCACATTTCTGA-3′
Genscan00000043157[c]	5′-GACAGTAGACTTCCCAGAGCACATAG-3′	5′-TCTCCTGTTTCAGTCCAATTCTGA-3′

[a] The position of ARE sites are described in Table 2.
[b] Primers for GAPDH coding were used for both ChIP assay and RT-PCR.
[c] Genscan00000043157: a putative transcript predicted by the Ensembl pipeline analysis system using the Genscan prediction program.

fluorescence. Primer pairs were designed by Primer Express ver. 2.0 software (Applied Biosystems), generating perfect ARE-containing fragments with the requirements of primer T_m temperature at basically 58–60 °C and the requirements of amplicon length for 50–150 bp. The protocol of PCR was 2 min at 50 °C, 10 min at 95 °C, and 40 cycles of 15 s at 95 °C and 1 min at 60 °C. To determine relative differences among the treatment groups for the chromatin immunoprecipitation (ChIP) assays we used the $\Delta\Delta C_t$ method as outlined in the Applied Biosystems protocol for reverse transcriptase-PCR. The average threshold cycle (C_t) for the duplicate was used in all subsequent calculations. A genomic fragment corresponding to GAPDH was used as an external standard. Genomic fragments containing proximal or distal ARE in the promoter region of prostate-specific antigen (PSA) (−250 to −39 bp and −4170 to −3978 bp from the transcriptional initiation site, respectively) [6] were used as positive controls. The sequences of the primers used in ChIP assays (synthesized by Sigma Genosys, Japan) are described in Table 1.

Quantitative reverse transcription-PCR. Total RNA was extracted from R1881-treated or 0.1% ethanol-treated LNCaP cells for 24 h using ISOGEN reagent (Nippon Gene, Tokyo, Japan). First strand cDNA was generated from RNase-free DNase I-treated total RNA by using SuperScript II Reverse Transcriptase (Invitrogen, Carlsbad, CA) and $pdT_{12\ 18}$ primer (Amersham Biosciences, Piscataway, NJ). Proximal genes or putative transcripts that locate within a ±20-kb distance from perfect AREs were selected for reverse transcription-PCR (RT-PCR) analysis. cDNAs were quantified by quantitative real-time PCR using the Applied Biosystems 7000 sequence detector based on SYBR Green I fluorescence as described above. The primer sequences for the amplifications are described in Table 1.

Results

In silico identification of perfect palindromic ARE sequences in the human genome

In terms of palindromic ARE sequences composed of two AGAACA sequences separated by a 3-bp spacer, a few near-consensus sequences, but no perfect palindromic sequences have been identified among human androgen-responsive genes. In order to answer the question whether perfect palindromic ARE sequences do function as in vivo AR binding sites, we computationally searched all the consensus ARE sequences in the human genome utilizing in-house Perl script and a program for regular expression pattern search of a nucleotide sequence in EMBOSS package (program name: dreg) [4]. The screening defined 563 elements, noting that the number of sites was larger than the expected frequency in random DNA sequences as calculated by the total number of base pairs in the genome divided by the frequency of a sequence with specified base pairs at 12 positions ($3{,}223{,}443{,}491/4^{12} = 192$). The distribution of consensus sequences among the chromosomes is generally consistent with chromosomal size, the average frequency of ARE being 17.3 ± 4.3 sites per 100 Mb (Figs. 1A and B).

In vivo AR recruitment of perfect AREs on chromosome X

To investigate whether the computationally identified ARE sequences with perfect motifs recruit AR in vivo,

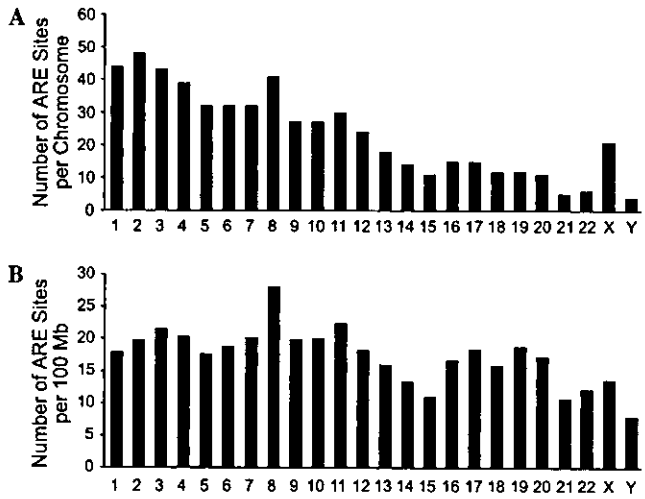

Fig. 1. Distribution of perfect palindromic AREs in the human genome. (A) The number of perfect consensus AREs found per chromosome. (B) The ratio between the number of perfect AREs and the length of chromosome (sites per 100 Mb).

we performed ChIP assay in AR-positive LNCaP cells. The chromosome X was selected as an experimental model, in which AR gene itself locates. The distribution of 21 perfect ARE sites on chromosome X is mapped in Fig. 2 and the detailed information of ARE (X1–X21) sites including nucleotide positions and sequences is in Table 2. None of the consensus AREs clustered in chromosome X within 50 kb, as the narrowest distance between X5 and X6 was 57.7 kb.

We performed quantitative PCR using genomic DNAs from LNCaP cells with 24-h treatment of R1881 (10 nM) or 0.1% ethanol, immunoprecipitated by either a specific AR antibody or non-specific rabbit IgG (Fig. 3). The AR association with proximal and distal promoter regions of PSA including ARE sequences was more than 3.5-fold and 60-fold increased by R1881 treatment, respectively. Of 21 genomic fragments containing perfect AREs in chromosome X, 8 fragments recruited more ARs (>4-fold enrichment) compared with the proximal ARE region of PSA. No particular specificity of 3-bp spacer sequences for AR recruitment has been found; for example, both ARE X5 and X6 sites contain a GCC spacer while fold enrichment of AR recruitment was 1.2-fold and 7.2-fold, respectively. In the case of X17 and X19 sites possessing an identical GCA spacer, fold difference of AR binding was 9.5-fold and 2.0-fold, respectively.

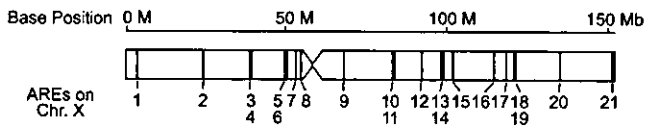

Fig. 2. Positions of the perfect palindromic AREs on chromosome X. Indicated numbers 1–21 correspond to perfect ARE sites.

Table 2
Proximal RNA transcripts in the vicinity of perfect palindromic AREs in chromosome X

AREID[a]	Start	Stop	ARE sequence	Proximal transcript	Ensembl ID No.	Location of ARE site[b]
X1	3181583	3181597	AGAACAtggTGTTCT	PRKX	ENSG00000183943	Within
X2	23945954	23945968	AGAACActaTGTTCT	PCYT1B	ENSG00000102230	Within
X3	38720672	38720686	AGAACAaagTGTTCT	*Ab-initio* Genscan transcript[c]	GENSCAN00000046001	Within
X4	38970910	38970924	AGAACAaagTGTTCT	BCOR	ENSG00000183337	5′ (3 kb)/within[d]
X5	49168004	49168018	AGAACAgccTGTTCT	*Ab-initio* Genscan transcript	GENSCAN00000107032	3′ (8 kb)
X6	49225713	49225727	AGAACAgccTGTTCT	*Ab-initio* Genscan transcript	GENSCAN00000043157	3′ (10 kb)
X7	52321185	52321199	AGAACAttaTGTTCT	O60275	ENSG00000124313	5′ (4 kp)
X8	53952953	53952967	AGAACAtaaTGTTCT	PFKFB1	ENSG00000158571	Within
X9	67507044	67507058	AGAACAgaaTGTTCT	*Ab-initio* Genscan transcript	GENSCAN00000115882	Within
X10	82472510	82472524	AGAACAatgTGTTCT	NM_144657	ENSG00000165259	Within
X11	83327890	83327904	AGAACAttcTGTTCT	NM_024921	ENSG00000124429	Within
X12	91506977	91506991	AGAACAaaaTGTTCT	*Ab-initio* Genscan transcript	GENSCAN00000029252	Within
X13	98772894	98772908	AGAACAagaTGTTCT	SYTL4	ENSG00000102362	5′ (5 kb)
X14	98951387	98951401	AGAACAtctTGTTCT	Ensembl novel transcript	ENST00000328526	Within
X15	101412450	101412464	AGAACAgctTGTTCT	NGFRAP1	ENSG00000166681	3′ (8 kb)
X16	114061336	114061350	AGAACAgaaTGTTCT	*Ab-initio* Genscan transcript	GENSCAN00000064921	Within
X17	118442517	118442531	AGAACAgcaTGTTCT	CUL4B	ENSG00000158290	Within
X18	120798222	120798236	AGAACActaTGTTCT	*Ab-initio* Genscan transcript	GENSCAN00000054945	Within
X19	121144935	121144949	AGAACAgcaTGTTCT	GRIA3	ENSG00000125675	Within
X20	134752049	134752063	AGAACAactTGTTCT	Q96NB7	ENSG00000173971	Within
X21	151348988	151349002	AGAACAcccTGTTCT	NM_152274	ENSG00000147382	5′ (16 kb)

[a] ARE ID X1–X21 correspond to the numbers 1–21 in Fig. 2.
[b] Location of ARE site indicates the proximity to annotated genes or putative transcripts.
[c] *Ab-initio* Genscan transcript: putative transcript predicted by the Ensembl pipeline analysis system using the Genscan prediction program [7].
[d] BCOR has two different initiation sites.

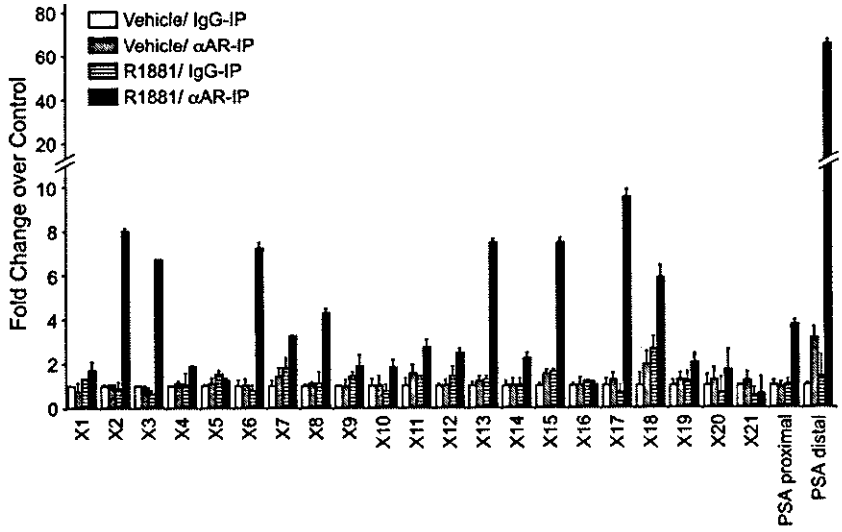

Fig. 3. Chromatin immunoprecipitation assay in LNCaP cells. Cells after 72-h hormone depletion were treated with 10 nM R1881 or 0.1% ethanol as a vehicle for 24 h. Quantitative PCR was performed using ChIP DNA samples immunoprecipitated by rabbit polyclonal anti-AR antibody (αAR-IP) or non-specific rabbit IgG (IgG-IP). In each case, fold enrichment values in R1881-treated samples immunoprecipitated by anti-AR antibody and non-specific rabbit IgG (R1881/αAR-IP and R1881/IgG-IP) as well as vehicle-treated ones precipitated by anti-AR antibody (vehicle/αAR-IP) were compared with those in vehicle-treated samples precipitated by non-specific rabbit IgG (vehicle/IgG-IP). Each result is the mean ± SEM of two independent experiments in duplication (four determinants). Prostate-specific antigen (PSA) proximal and distal promoter regions are served as positive controls.

Potential transcriptional regulation of proximal genes in the vicinity of perfect AREs

To examine whether perfect AREs regulate transcriptional activities of proximal genes, we next performed quantitative RT-PCR for RNA transcripts in the vicinity of consensus ARE sites. Proximal genes were selected for each ARE site based on the following requirements of ARE location: (1) within an annotated gene, (2) within 20-kb upstream to 5′ end of a known gene, or (3)

within 20-kb downstream to 3′ terminus of a known gene (Table 2). If no annotated genes exist in the vicinity of ARE sites, putative transcripts predicted by the Ensembl pipeline analysis system using the Genscan prediction program [7] and mapped on the Ensembl genome browser were chosen (i.e., *ab-initio* Genscan transcripts). Ten out of 21 AREs are located within introns of known genes or a novel transcript, 4 sites in the 5′ regions of annotated genes [ARE X4 is counted in both 5′ region and within intron 1 of BCOR (BCL-6 interacting corepressor) due to variants], one site in the 3′ regions of a known gene. No known genes were found in the vicinity of seven ARE sites.

Quantitative RT-PCR was conducted using the first-strand cDNAs derived from LNCaP cells treated with a synthetic androgen R1881 or 0.1% ethanol as a vehicle for 24 h. Two annotated genes and one putative transcript exhibited significant increase in transcript expression levels agonist-dependently (Fig. 4). PCYT1B (phosphorylcholine transferase B) is a gene encoding an enzyme that controls phosphatidylcholine synthesis [8,9]. PCYT1B may be related to the reproduction function as it is highly expressed in testis, placenta, and ovary. Perfect ARE (X2) locates within intron 7 of PCYT1B. In regard to NM_144657, the gene encodes 690 amino acids and contains perfect ARE (X10) within intron 3. Although the fold enrichment of R1881-activated AR binding in ARE X10 was smaller than that in the PSA proximal promoter region, yet it is statistically significant ($P < 0.05$). The gene NM_144657 is found to possess two HOX homeobox domains by analyzing domain architectures using a Simple Modular Architecture Research Tool (SMART) on InterPro databases (http://www.ebi.ac.uk/interpro/databases.html). The gene may be a nuclear DNA-binding protein that is involved in the transcriptional regulation of developmental processes. Concerning an *ab-initio* Genscan transcript (ID: Genscan00000043157) that is located 10-kb upstream to consensus ARE (X6), the sequence does not exhibit overall similarity with any characterized human gene.

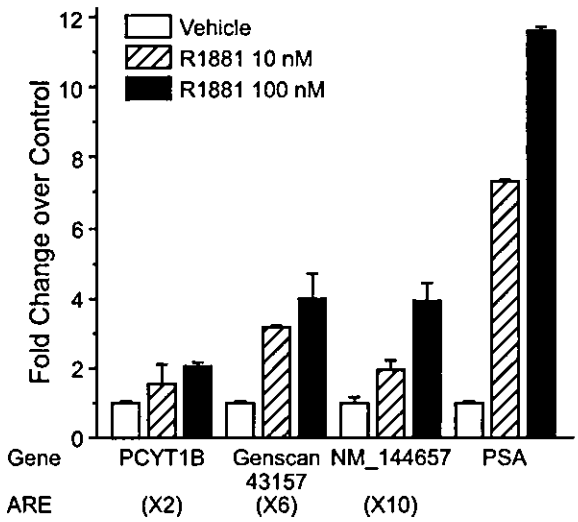

Fig. 4. Quantitative RT-PCR of proximal genes in the vicinity of perfect AREs. LNCaP cells after 72-h hormone depletion were treated with R1881 (10 or 100 nM) or 0.1% ethanol as a vehicle for 24 h. Real-time PCR was conducted using the first strand cDNAs generated from the total RNAs of the cells. PCYT1B, Genscan43157 (Genscan00000043157), and NM_144657 are located in the vicinity of ARE X2, X6, and X10, respectively. Each result is the mean ± SEM of two independent experiments in duplication (four determinants). PSA is served as a positive control.

Discussion

In the present study, we identified 563 perfect palindromic ARE sequences in the human genome, whose frequency of occurrence is more than our initial expectation of approximately 200 sites. We functionally analyzed 21 consensus AREs on chromosome X as a sample of the population. Eight of 21 AREs recruited more ARs (>4-fold enrichment) upon ligand treatment even compared with the proximal ARE region of PSA, as determined by ChIP assay using human prostate cancer LNCaP cells. It was also shown that distal ARE region of PSA showed by far the highest recruitment of AR. In regard to the expression of transcripts that locate with ±20 kb from perfect AREs, two annotated genes and one putative transcript were upregulated ligand-dependently, suggesting that these proximal genes are potentially androgen-responsive genes.

Our results reveal two interesting points in the field of steroid receptors. One is the frequency of occurrence of hormone response elements. Based on our data of ChIP assay along chromosome X, there might be at least 200 perfect ARE sequences that actually function as AR binding sites in the entire human genome. A recent computational analysis of near-consensus estrogen response elements, in which 10 specified nucleotides and 2 nucleotide choices at 2 positions out of 12 bp, revealed that there are approximately 70,000 sequences in the human and mouse genomes [10]. By the experimental approach of tiling array of chromosomes 21 and 22 hybridized with immunoprecipitated DNAs, there might be large number of transcription factor binding sites with a minimal estimate of 12,000 for Sp1, 25,000 for c-Myc, and 1600 for p53 [11]. Taking together our present results and the estimation of transcription factors by others, there may be at least several thousand sites of functional AREs in the human genome.

The second interesting point is the relationship of perfect AREs to proximal genes and potential transcription regulation by consensus AREs. In our results, nearly half of the perfect AREs (10 of 21) on chromosome X are located within introns of annotated genes

including one novel transcript. The frequency of AREs within known genes is much higher than that of AREs in 5′ regions of annotated genes (4 of 21). In the case of transcription factor binding sites on chromosomes 21 and 22, 36% of these regions are situated within known genes or proximal to the 3′ most exon of a gene and the frequency was also higher than that of binding sites within 5′ to known genes (22%) [11]. As for NF-κB binding sites on chromosome 22, 40% of the regions are located in intronic sequences [12]. Indeed, there is evidence that several intronic DNA elements for NF-κB are functionally important in the gene regulation by co-operating with other DNA elements [13,14]. Thus, some of the consensus ARE sequences within annotated genes may be functional in the transcriptional regulation of those genes. Yet, those intronic binding sites are interesting in terms of the potential for distal regulatory elements or promoters for non-coding transcripts or antisense transcripts overlapping the 3′ untranslated regions.

In regard to consensus ARE sequences in unannotated regions, 7 of 21 sites are in regions more than ±20 kb apart from any annotation or novel transcribed regions. Six of 7 sites in unannotated regions are located within regions corresponding to *ab-initio* Genscan transcripts. The remaining one site (X6) is situated at 10-kb downstream to the 3′ end of an *ab-initio* Genscan transcript, yet this ARE may be functional as it has a significant in vivo AR binding ability and the expression levels of the proximal *ab-initio* Genscan transcript (Genscan00000043157) are androgen-inducible. It is interesting to compare our results with NF-κB binding sites on chromosome 22 [12], as 22% of the binding sites for p65 lie in regions more than 50 kb from any annotation. Taken together, our results suggest that there are many unannotated regions that include transcription factor binding sites and have biological functions.

Concerning the differences in binding potency among AREs, several factors such as the nearby chromosomal environment or the chromatin accessibility of specific co-operating factors as well as basal transcriptional factors may be involved. Future comparative studies with different cell context will reveal the variations of chromatin structure and contribute to the identification of novel androgen-responsive genes that are critically involved in the development of prostate cancer.

In summary, the present study demonstrates the usefulness of the genome-wide approach combined with computational analysis and experimental verification in hormone-responsive genes. Our functional analysis reveals that some of the perfect AREs are actual AR binding sites in vivo and may relate to the transcription regulation of proximal genes. Our study will mark the first step toward the elucidation of the entire gene regulatory network mediated by androgen.

Acknowledgments

We thank Y. Suzuki and R. Nozawa for their technical assistance. This work was supported by Grants-in-Aid for Scientific Research under Category "S" and Scientific Research in Priority Areas "Cancer Research" and "Genome Science" from the Ministry of Education, Culture, Sports, Science and Technology of Japan.

References

[1] P.S. Nelson, N. Clegg, H. Arnold, C. Ferguson, M. Bonham, J. White, L. Hood, B. Lin, The program of androgen-responsive genes in neoplastic prostate epithelium, Proc. Natl. Acad. Sci. USA 99 (2002) 11890–11895.

[2] P.L. Shaffer, A. Jivan, D.E. Dollins, F. Claessens, D.T. Gewirth, Structural basis of androgen receptor binding to selective androgen response elements, Proc. Natl. Acad. Sci. USA 101 (2004) 4758–4763.

[3] E. Birney, D. Andrews, P. Bevan, M. Caccamo, G. Cameron, Y. Chen, L. Clarke, G. Coates, T. Cox, J. Cuff, et al., Ensembl 2004, Nucleic Acids Res. 32 (2004) D468–D470.

[4] P. Rice, I. Longden, A. Bleasby, EMBOSS: the european molecular biology open software suite, Trends Genet. 16 (2000) 276–277.

[5] V. Matys, E. Fricke, R. Geffers, E. Gossling, M. Haubrock, R. Hehl, K. Hornischer, D. Karas, A.E. Kel, O.V. Kel-Margoulis, et al., TRANSFAC: transcriptional regulation, from patterns to profiles, Nucleic Acids Res. 31 (2003) 374–378.

[6] Y. Shang, M. Myers, M. Brown, Formation of the androgen receptor transcription complex, Mol. Cell 9 (2002) 601–610.

[7] C. Burge, S. Karlin, Prediction of complete gene structures in human genomic DNA, J. Mol. Biol. 268 (1997) 78–94.

[8] A. Lykidis, I. Baburina, S. Jackowski, Distribution of CTP:phosphocholine cytidylyltransferase (CCT) isoforms. Identification of a new CCT splice variant, J. Biol. Chem. 274 (1999) 26992–27001.

[9] A. Lykidis, K.G. Murti, S. Jackowski, Cloning and characterization of a second human CTP:phosphocholine cytidylyltransferase, J. Biol. Chem. 273 (1998) 14022–14029.

[10] V. Bourdeau, J. Deschenes, R. Metivier, Y. Nagai, D. Nguyen, N. Bretschneider, F. Gannon, J.H. White, S. Mader, Genome-wide identification of high-affinity estrogen response elements in human and mouse, Mol. Endocrinol. 18 (2004) 1411–1427.

[11] S. Cawley, S. Bekiranov, H.H. Ng, P. Kapranov, E.A. Sekinger, D. Kampa, A. Piccolboni, V. Sementchenko, J. Cheng, A.J. Williams, R. Wheeler, B. Wong, J. Drenkow, M. Yamanaka, S. Patel, S. Brubaker, H. Tammana, G. Helt, K. Struhl, T.R. Gingeras, Unbiased mapping of transcription factor binding sites along human chromosomes 21 and 22 points to widespread regulation of noncoding RNAs, Cell 116 (2004) 499–509.

[12] R. Martone, G. Euskirchen, P. Bertone, S. Hartman, T.E. Royce, N.M. Luscombe, J.L. Rinn, F.K. Nelson, P. Miller, M. Gerstein, S. Weissman, M. Snyder, Distribution of NF-κB-binding sites across human chromosome 22, Proc. Natl. Acad. Sci. USA 100 (2003) 12247–12252.

[13] H. Schjerven, P. Brandtzaeg, F.E. Johansen, A novel NF-κB/Rel site in intron 1 cooperates with proximal promoter elements to mediate TNF-α-induced transcription of the human polymeric Ig receptor, J. Immunol. 167 (2001) 6412–6420.

[14] K. Maehara, T. Hasegawa, K.I. Isobe, A NF-κB p65 subunit is indispensable for activating manganese superoxide: dismutase gene transcription mediated by tumor necrosis factor-α, J. Cell. Biochem. 77 (2000) 474–486.

Laboratory Investigation (2004) 84, 1460–1471

www.laboratoryinvestigation.org

Estrogen receptor-associated expression of keratinocyte growth factor and its possible role in the inhibition of apoptosis in human breast cancer

Naóe Tamaru[1,2], Yoshitaka Hishikawa[1], Kuniaki Ejima[1], Naofumi Nagasue[3], Satoshi Inoue[4], Masami Muramatsu[4], Tomayoshi Hayashi[2] and Takehiko Koji[1]

[1]*Division of Histology and Cell Biology, Department of Developmental and Reconstructive Medicine, Nagasaki University Graduate School of Biomedical Science, Nagasaki, Japan;* [2]*Department of Pathology, Nagasaki University Hospital, Nagasaki, Japan;* [3]*Second Department of Surgery, Shimane Medical University, Izumo, Japan and* [4]*Future Program Research Division, Saitama Medical School, Saitama, Japan*

Although estrogen is known to play a crucial role in the pathogenesis of breast cancer, the molecular mechanisms underlying the action of estrogen remain elusive. In the present study, we focused on keratinocyte growth factor (KGF) and its receptor (KGFR) in the pathogenesis of breast cancer, as a growth factor mediating estrogen action, since significant roles of KGF were demonstrated in various steroid hormone-dependent tissues. First, using paraffin-embedded specimens from 42 breast cancer patients, we examined expression patterns of KGF and KGFR by both immunohistochemistry using newly generated antibodies and nonradioactive *in situ* hybridization with T–T dimerized synthetic oligonucleotide probes. We next compared the results with the expression of estrogen receptor (ER) α and β, proliferative activity and apoptotic frequency (TUNEL staining). Also, the similar approaches were taken to analyze the expression and role of KGF in ER-positive (MCF7, ZR-75-1) and ER-negative (SK-BR-3, MDA-MB-231) human breast cancer cell lines *in vitro*. In the surgical specimens, KGF was expressed in cancer cells as well as stromal cells in 19/42 cases (45%), while KGFR was found in cancer cells in 24/42 cases (57%). The distribution of protein and mRNA in the analysis of both KGF and KGFR expression generally coincided. Moreover, KGF expression was closely associated with the expression of ER α, and the coexpression of KGF and KGFR significantly correlated with lower TUNEL index, but not with proliferative activity. In accordance with the *in vivo* findings, KGF expression was detected only in ER α-positive MCF7 and ZR-75-1 cells *in vitro*. And more importantly, we found the inhibitory effect of KGF upon the induction of apoptosis by anticancer drugs in MCF7 cells. Collectively, our results indicate that ER α may be involved in KGF expression, and that KGF may play antiapoptotic roles, rather than mitogenic, in human breast cancer.
Laboratory Investigation (2004) **84,** 1460–1471, advance online publication, 16 August 2004; doi:10.1038/labinvest.3700166

Keywords: apoptosis; breast cancer; estrogen receptor; immunohistochemistry; *in situ* hybridization; keratinocyte growth factor; TUNEL staining

Breast cancer is the most frequent malignant tumor of women in the USA and European countries. In Japan, the frequency of breast cancer has rapidly increased during the last decade, and currently approximately 20 000 women develop breast cancer per year. However, our knowledge of the development and progression of breast cancer is still largely limited. The proliferation and differentiation of breast cancer cells are influenced by estrogen,[1–3] which exerts its action through binding to estrogen receptor (ER). Currently, ER is categorized into two subtypes, ER α and β, and both are believed to act as an active transcription factor, which binds to a specific DNA segment such as the estrogen responsive element (ERE) and AP-1 site, to regulate the expression of a variety of genes.[4,5] The majority of human breast cancer cells express both ER α and ER β.[6] While ER α is regarded as an indicator of

Correspondence: Professor T Koji, PhD, Division of Histology and Cell Biology, Department of Developmental and Reconstructive Medicine, Nagasaki University Graduate School of Biomedical Science, 1-12-4 Sakamoto, Nagasaki 852-8523, Japan.
E-mail: tkoji@net.nagasaki-u.ac.jp
Received 27 October 2003; revised 9 July 2004; accepted 11 July 2004; published online 16 August 2004

good prognosis,[6] the correlation of ER β expression with tamoxifen-sensitivity and prognosis is highly controversial.[6–8]

Several locally synthesized polypeptide growth factors and their receptors are known to interact with estrogen in the pathogenesis of breast cancer. For example, expression of transforming growth factor-α is induced by estrogen and stimulates proliferation of breast cancer cells.[9,10] On the other hand, HER2 (erbB-2), known as a marker of poor prognosis in human breast cancer,[11,12] is down-regulated by estrogen in an ER-dependent fashion.[12,13] However, the role of growth factors in the pathogenesis of breast cancer, including their interactions with estrogen, is very complicated and largely unclarified. Keratinocyte growth factor (KGF), also known as fibroblast growth factor (FGF)-7, was originally discovered by Rubin *et al*[14] as a unique member of the FGF family. KGF appeared to be synthesized and secreted by stromal cells and to act on epithelial cells specifically through a high-affinity receptor for KGF (KGFR).[14–16] Therefore, KGF is considered to be a unidirectional paracrine effector that regulates normal epithelial cell proliferation.[15] In particular, KGF appears to be an essential mediator of steroids in various reproductive organs as andromedin[17] and progestomedin.[18] Indeed, KGF mRNA was detected in isolated stromal cells from human breast cancer[19,20] and was upregulated by estrogen.[20] However, there was a significant variation in the level of KGF mRNA, and the significance of its expression in breast cancer tissue remains highly controversial.[19,20] Moreover, KGF is known to have diverse effects, such as inhibition of apoptosis[21–23] and regulation of cell differentiation.[24–26] To help clarify these issues, it is desirable to localize KGF and KGFR at a cellular level in tissue sections of human breast cancer. Although KGF mRNA expression in ruminant mammary gland was previously detected by *in situ* hybridization using autoradiography,[27] there have been no reports on immunohistochemical analysis of KGF and KGFR expression in human breast cancer tissue. Considering that the state of mRNA preservation in human surgical specimens can vary considerably,[28] the analysis of protein expression by immunohistochemistry might yield more convincing information. However, mainly because of the lack of reliable antibodies for KGF and KGFR, studies of KGF and KGFR proteins have been limited.

The present study was designed to assess the significance of KGF and KGFR expression in the pathogenesis of human breast cancer. For this purpose, we localized KGF and KGFR in surgical specimens of human breast cancer using newly prepared antibodies for them. Furthermore, expression of KGF and KGFR was examined at the mRNA level by *in situ* hybridization. We then compared the KGF and/or KGFR expression with ER α and β expression, proliferative activity, and the frequency of apoptosis. We also investigated the association between ERs and KGF expressions and the effect of KGF on the induction of apoptosis in breast cancer cells *in vitro*. As a result, in surgical specimens, KGF and KGFR were detected in cancer cells and KGF expression was tightly associated with ER α expression. Moreover, coexpression of KGF and KGFR significantly correlated with lower frequency of apoptosis *in vivo*. In addition, we detected KGF expression only in ER α-positive breast cell lines, but not in ER α-negative ones. Also, it was found that KGF significantly decreased the frequency of apoptotic cells induced by anticancer drugs in MCF7 cells. These results indicate that KGF expression in breast cancer cells may depend upon the presence of ER α, and that KGF may play an inhibitory role in the induction of breast cell apoptosis in an autocrine and/or paracrine manner.

Materials and methods

Biochemicals and Chemicals

Paraformaldehyde was purchased from Merck (Darmstadt, Germany). 3,3′-diaminobenzidine/4HCl (DAB) and ethylenediaminetetraacetic acid was purchased from Dojin Laboratories (Kumamoto, Japan). Mixed-bed resin (AG501-X8 (D) Resin 20–50 mesh) was purchased from Bio-Rad Laboratories (Tokyo, Japan). Proteinase K, bovine serum albumin (BSA, minimum 98%, electrophoresis), yeast transfer RNA (type X-SA), salmon testis DNA, dextran sulfate, polyadenylic acid, heparin, Brij 35, Triton X-100, 3-aminopropyltriethoxysilane, 17β-estradiol, cyclophosphamide, and 5-fluorouracil were purchased from Sigma Chemical Co. (St Louis, MO, USA). Formamide (nuclease and protease free) was purchased from Nacalai Tesque (Kyoto, Japan). Biotin-16-dUTP and terminal deoxynucleotidyl transferase (TdT) were from Roche (Mannheim, Germany). RPMI 1640 was from Invitrogen (Carlsbad, CA, USA). Dextran-coated charcoal-treated fetal bovine serum was from ThermoTrace (Melbourne, Australia). Penicillin potassium and streptomycin sulfate were purchased from Meiji, Ltd. (Tokyo, Japan). Recombinant human KGF was from Peprotech (London, UK). Hoechst 33342 dye was from Calbiochem (La Jolla, CA, USA). All other reagents used in this study were purchased from Wako Pure Chemicals (Osaka, Japan) and were of analytical grade.

Antibodies for KGF and KGFR

Polyclonal antibodies against KGF and KGFR were prepared by immunization of rabbits against synthetic peptides in cooperation with Nichirei Co. (Tokyo, Japan) as previously described.[29] For immunohistochemical analysis, anti-KGF antibody

(5 μg/ml) and anti-KGFR antisera (1:600) were used to identify KGF or KGFR expression, respectively, which yielded the highest signal/noise ratio in paraffin-embedded sections of human breast cancer tissues.

Other Antibodies

A mouse monoclonal antibody against human ER α (0.3 μg/ml) was purchased from DAKO (Glostrup, Denmark). A mouse monoclonal antibody against human Ki-67 (0.5 μg/ml) was purchased from Immunotech (Marseille, France). Rabbit anti-human ER β antiserum (1:400) was generated as previously described[30,31] and kindly provided by Dr Muramatsu (Future Program Research Division, Saitama Medical School). Horseradish peroxidase (HRP)-conjugated goat anti-rabbit IgG F (ab)' (1:200) was purchased from MBL (Nagoya, Japan). HRP-goat anti-mouse IgG F (ab)' (1:200) was purchased from Chemicon International (Temecula, CA, USA). HRP-mouse anti-T-T antibody (1:80) was obtained from Kyowa Medex (Shizuoka, Japan). HRP-goat anti-biotin antibody (1:100) was from Vector Laboratories (Burlingame, CA, USA). Normal goat IgG, normal rabbit IgG, and normal mouse IgG were from Sigma Chemical Co. Normal goat serum and normal rabbit serum were purchased from DAKO.

Tissue Collection and Preparation

In all, 42 cases of human breast cancer tissues were surgically resected from 1998 to 2001 and diagnosed histologically as carcinoma. Totally, 36 cases were invasive ductal carcinoma, six cases were invasive lobular carcinoma. All patients were female, the average age was 55.7 ± 13.9 years, and did not have preoperative tamoxifen treatment. All patients or their next of kin provided informed consent for participation in the clinical study. The tissues were fixed with 4% paraformaldehyde in PBS and embedded in paraffin. Serial sections were cut at 5 μm thickness and then placed onto 3-aminopropyltriethoxysilane-coated glass slides.

Cell Culture

MCF7, ZR-75-1 and SK-BR-3 were obtained from Cell Resource Center for Biomedical Research Institute of Development, Aging and Cancer, Tohoku University (Sendai, Japan). MDA-MB-231 was purchased from ATCC (Manassas, VA, USA). For the analysis of KGF expression, cells were incubated for 1 week in phenol-red free RPMI 1640 medium, supplemented with 100 U/ml penicillin potassium, 100 μg/ml streptomycin sulfate, and 10% dextran-coated charcoal-treated fetal bovine serum at 37°C and 5% CO_2. The cells were further incubated in the chamber slides (Lab-Tek, Nalge Nunc International, Naperville, IL, USA) in the absence or presence of 10 nM 17β-estradiol for 2 more days. After fixation with 4% paraformaldehyde in PBS for 10 min at RT, the slides were subjected to enzyme immunohistochemistry. For the analysis of the antiapoptotic effect of KGF, the cells were incubated for 1 day in RPMI 1640 medium supplemented with the antibiotics and 0.1% dextran-coated charcoal-treated fetal bovine serum at 37°C and 5% CO_2. Then 25 μg/ml 5-fluorouracil or 500 μg/ml cyclophosphamide were added with or without 10 ng/ml recombinant human KGF and further incubated for 2 days. After fixation with 4% paraformaldehyde in PBS, the staining with Hoechst 33342 was performed and the frequency of cells with nuclear fragmentation as an indicator of apoptosis was calculated.[32]

Immunohistochemistry

Enzyme immunohistochemistry was performed to examine the expression of KGF, KGFR, ER α, ER β, and Ki-67 in breast cancer tissue. Paraffin sections of breast cancer were deparaffinized with toluene and rehydrated with serially graded ethanol solutions. For KGFR, the sections were immersed in 0.2% Triton X-100 in PBS for 10 min at room temperature (RT). The sections were autoclaved at 121°C for 15 min (for ER α and Ki-67) or microwaved at 95°C for 20 min (for ER β) in 10 mM citrate buffer (pH 6.0). After inactivation of endogenous peroxidase activity with 0.3% H_2O_2 in methanol for 15 min at RT, the sections were preincubated with blocking solution for 1 h at RT. For KGFR and ER β, 10% normal goat serum and 1% BSA in PBS was used as a blocking solution. For the others, 500 μg/ml normal goat IgG and 1% BSA in PBS was used. The sections were then incubated with the first antibodies for 2 h (KGF and KGFR) or overnight (ER α, ER β, and Ki-67) at RT. After incubation, slides were washed 3 times with 0.075% Brij 35 in PBS. Then sections were reacted with HRP-goat anti-rabbit IgG (1:200) or HRP-goat anti-mouse IgG (1:200) for 1 h at RT and washed 3 times with 0.075% Brij 35 in PBS. HRP sites were visualized with H_2O_2 and DAB solution[33] or H_2O_2 and DAB in the presence of nickel and cobalt ions.[34] As a negative control, normal rabbit IgG, normal rabbit serum, or normal mouse IgG was used instead of the first antibody in each run. For colocalization of ERs and KGF, the sections were stained with anti-KGF antibody according to the protocol described above, and HRP sites were visualized with H_2O_2 and DAB solution. Then the sections were immersed in PBS and autoclaved in 10 mM citrate buffer (pH 6.0) for 15 min at 121°C for 15 min. The sections were immersed in 0.1 M glycine-HCl buffer (pH 2.2) for 30 min 3 times, and rinsed with Milli-Q water once and immersed in PBS. Then the sections were stained with anti-ER antibody, as described above. HRP sites were

visualized with H_2O_2 and 4-chloro-1-naphthol solution.[35]

Probes and Labeling

Sense and antisense oligo-DNA sequences corresponding to nucleotides No. 648–683 of the human KGF cDNA sequence[15] and nucleotides No. 1388–1432 of the human KGFR cDNA[16] were synthesized on a DNA synthesizer. These 36- and 45-base oligo-DNAs were added with two repeats of adenine–thymine–thymine at the 5′ ends, and two or three repeats of it at the 3′ ends of 36-base oligo-DNAs and 45-base oligo-DNAs, respectively, for thymine–thymine (T–T) dimers.[36] We conducted a computer-assisted search (GenBank nucleic acid sequence database Release 129) of the above KGF and KGFR oligo-DNA sequences (without adenine–thymine–thymine repeats) and found 100% homology with those mRNA sequences. These KGF and KGFR oligo-DNAs were haptenized by introducing T–T dimers by 12 000 J/m^2 ultraviolet irradiation, as described previously.[36,37] We performed preliminary immunodetection and dot-blot hybridization using KGF and KGFR probes as detailed previously,[37,38] and these results indicated that antisense probes were specific and had adequate sensitivity to be useful for *in situ* hybridization.

In Situ Hybridization

In situ hybridization was performed as described previously.[18] Briefly, paraffin sections of breast cancer were deparaffinized with toluene and rehydrated using serially graded ethanol solutions. The slides were treated with 0.2 N HCl for 20 min, 0.2% Triton X-100 in PBS for 10 min, and proteinase K (25 μg/ml, 37°C, for 15 min), successively. After the slides were postfixed with 4% paraformaldehyde in PBS, they were immersed twice in 2 mg/ml glycine in PBS for 15 min. Hybridization was carried out at 37°C for KGF and 42°C for KGFR overnight in a medium containing 10 mM Tris-HCl (pH 7.4), 1 mM ethylenediaminetetraacetic acid, 0.6 M NaCl, 1 × Denhardt's solution, 250 μg/ml yeast transfer RNA, 125 μg/ml salmon testis DNA, 10% dextran sulfate, 200 U/ml heparin, 10 μg/ml polyadenylic acid potassium salt, 40% deionized formamide, and 2 μg/ml T–T dimerized KGF probe or T–T dimerized KGFR probe. After hybridization, the slides were washed 3 times with 2 × SSC/50% formamide/0.075% Brij 35 at 37°C, twice with 0.5 × SSC/50% formamide/0.075% Brij 35 at 37°C for 1 h each, and finally washed twice with 2 × SSC at RT for 15 min. The slides were subjected to enzyme immunohistochemistry. After incubation with blocking solution (5% BSA, 0.3 M NaCl, 100 μg/ml salmon testis DNA, 100 μg/ml yeast transfer RNA, and 500 μg/ml normal mouse IgG in PBS) for 1 h at RT, the slides were reacted overnight with HRP-mouse anti-T-T antibody (1:80) at RT. After washing with 0.075% Brij 35 in PBS, visualization of HRP sites was performed with H_2O_2 and DAB in the presence of nickel and cobalt ions, according to the method of Adams.[34] Positive cells were evaluated based on the staining density over the level of staining with the sense probe using an image analyzer (DAB system; Carl Zeiss, Göttingen, Germany). To confirm the specificity of mRNA signals, a variety of control experiments were conducted. In every run, sense probe was used as a negative control. To evaluate the level of hybridizable RNAs in tissue sections, a 28S rRNA probe was used as a positive control in every case.[28] Furthermore, some sections were hybridized with antisense probe in the presence of an excess amount of unlabeled antisense or unlabeled sense probe to provide definitive evidence for the sequence specificity of the signal as described previously in detail.[38]

TUNEL Staining

To analyze internucleosomal DNA fragmentation as a hallmark of apoptosis, TUNEL was carried out according to the method of Gavrieli *et al*[39] with a slight modification. Briefly, the sections were deparaffinized with toluene and rehydrated in serially graded ethanol solutions. After washing with PBS, the sections were treated with proteinase K (0.1 μg/ml, for 15 min at 37°C) and rinsed once with distilled water. The sections were incubated with 1 × TdT buffer (25 mM Tris-HCl buffer, pH 6.6, containing 0.2 M potassium cacodylate and 0.25 mg/ml BSA) alone for 30 min at RT. The sections were then reacted with 200 U/ml TdT dissolved in TdT buffer supplemented with 5 μM biotin-16-dUTP, 20 μM dATP, 1.5 mM $CoCl_2$, and 0.1 mM dithiothreitol for 90 min at 37°C. The reaction was terminated by washing with 50 mM Tris-HCl buffer (pH 7.4) and endogenous peroxidase activity was inhibited by immersing the slides in 0.3% H_2O_2 in methanol for 15 min at RT. After incubation with 500 μg/ml normal goat IgG in 5% BSA in PBS for 1 h at RT, the sections were reacted with HRP-goat anti-biotin antibody (1:100, diluted with 5% BSA in PBS) overnight at RT. After washing with 0.075% Brij 35 in PBS, the HRP sites were visualized with H_2O_2 and DAB in the presence of nickel and cobalt ions according to the method of Adams.[34] As a negative control, some sections were subjected to reaction without TdT.

Quantitative Analysis

The results of immunohistochemistry for KGF, KGFR, Ki-67, ER α, and ER β were graded as positive or negative, compared with the staining with IgG or serum of normal rabbit or mouse. For quantitative analysis, more than 2000 cancer cells were counted

in random fields at ×400 magnification, and the number of Ki-67-positive cancer cells was expressed as a percentage of positive cells per total number of counted cancer cells (Ki-67 labeling index (LI); mean ± s.d.). The percentage of apoptotic cells (TUNEL-positive cells or cells with nuclear fragmentation) was calculated in the same manner as for the Ki-67 LI.

Statistical Analysis

All data for Ki-67 LI and frequency of apoptosis (TUNEL index or frequency of cells with nuclear fragmentation) were expressed as mean ± s.d. Differences in Ki-67 LI or frequency of apoptosis were examined for statistical significance using the unpaired Student's *t*-test. Correlation between ER

Figure 1 Immunohistochemical detection of KGF and KGFR in paraffin sections of normal breast tissue (**a**, **b**) and breast cancer (**c–f**). (**a**) KGF was not detected in normal breast tissue. (**b**) KGFR was not detected in normal breast tissue. (**c**) KGF-positive cells were detected in the tumor nest and in the stroma. (**d**) KGFR-positive cells were found in the tumor nest. (**e**) Normal rabbit IgG was used instead of anti-KGF antibody. (**f**) Normal rabbit serum was used instead of anti-KGFR antibody. Arrows = positive cells. Magnification, ×100.

expression and KGF and/or KGFR expression was examined using χ^2 analysis. A *P*-value of less than 0.05 denoted the presence of a statistically significant difference. All analyses were performed with a statistical software package (StatView, version J 5.0; Abacus Concepts, Berkeley, CA, USA).

Results

Localization of KGF and KGFR in Normal Breast Tissue and Breast Cancer

KGF (Figure 1a) and KGFR (Figure 1b) were not detected by immunohistochemistry in normal breast tissue. In breast cancer tissue, however, KGF protein was detected in the cytoplasm of cancer cells and stromal cells (Figures 1c and 2a). On the other hand, KGFR was exclusively detected in the plasma membrane and cytoplasm of cancer cells (Figures 1d and 2f). When sections were reacted with normal rabbit IgG or serum, respectively, instead of the first antibody, no staining was found (Figure 1e and f).

To confirm the expression of KGF and KGFR mRNAs in breast cancer, we performed *in situ* hybridization. RNA preservation in all specimens was evaluated by methyl green/pyronin Y staining,[40] and 23 cases with well-preserved RNA were selected for *in situ* hybridization. As shown in Figure 2, KGF mRNA was detected in the cytoplasm of cancer cells and stromal cells (Figure 2b and c), which was consistent with the results of immunohistochemistry (Figure 2a). KGFR mRNA was detected in the cytoplasm of cancer cells (Figure 2g and h), and the distribution of KGFR mRNA generally coincided with that of KGFR protein (Figure 2f–h). To verify the specificity of the KGF and KGFR mRNA signals, we conducted various control experiments. When hybridized with KGF (Figure 2d) and KGFR (Figure 2i) sense probes, the staining was markedly reduced compared to that with KGF and KGFR antisense probes. Similarly, when adjacent sections were hybridized with KGF and KGFR antisense probes in the presence of a 100-fold excess amount of unlabeled corresponding antisense oligo-DNA, KGF and KGFR mRNA signal was markedly decreased (Figure 2e and j). In the present study, 19 of 42 (45%) breast cancers expressed KGF protein in cancer cells and/or stromal cells. The number of KGFR-positive cases was 24 of 42 (57%). In total, 10 cases (24%) were KGF- and KGFR-negative, 13 cases (31%) were KGF-negative but KGFR-positive, eight cases (19%) were KGF-positive but KGFR-negative, and 11 cases (26%) were both KGF- and KGFR-positive.

Correlation between ER Expression and KGF and/or KGFR Expression

We examined the expression of ER α and/or β and their correlation with KGF and KGFR expression in breast cancer. ER α was detected in the nuclei of cancer cells in 29 of 42 (69%) cases (Figure 3a). ER β was detected in the nuclei of cancer cells in 36 of 42 (86%) cases (Figure 3b). In total, two cases were both ER α- and β-negative, 11 cases were ER α-negative, but ER β-positive, four cases were ER α-positive, but

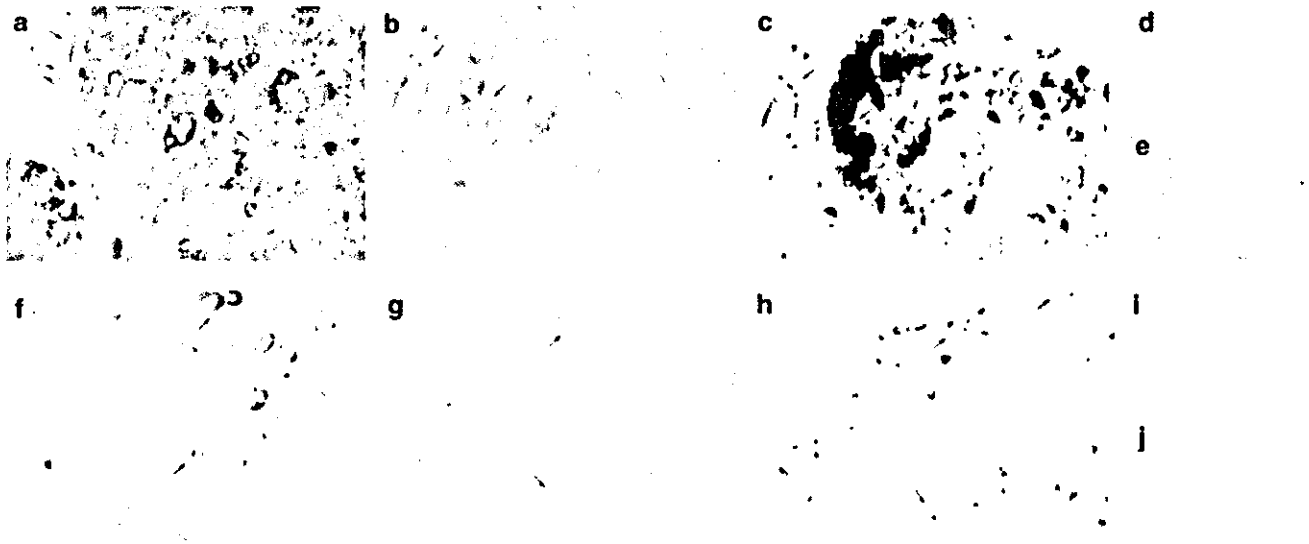

Figure 2 Immunohistochemistry and *in situ* hybridization for KGF and KGFR in breast cancer tissue. **(a)** Immunohistochemistry for KGF. KGF-positive cells were found in the tumor nest and in the stroma. **(b)** Section hybridized with KGF antisense probe. **(c)** Section hybridized with KGF antisense probe (the same section as **(b)**) was subjected to an image analyzer. The red color was assigned to positive cells. **(d)** Section hybridized with KGF sense probe. **(e)** Section hybridized with KGF antisense probe in the presence of an excess amount of unlabeled antisense probe. Red-colored positive cells were obviously fewer compared with **(c)**. **(f)** Immunohistochemistry for KGFR. **(g)** Section hybridized with KGFR antisense probe. **(h)** Section hybridized with KGFR antisense probe (the same section as **(g)** was subjected to an image analyzer. The red color was assigned to positive cells. **(i)** Section hybridized with KGFR sense probe. **(j)** Section hybridized with KGFR antisense probe in the presence of an excess amount of unlabeled antisense probe. No positive cells were found. Arrows = positive cells. Magnification, × 100.

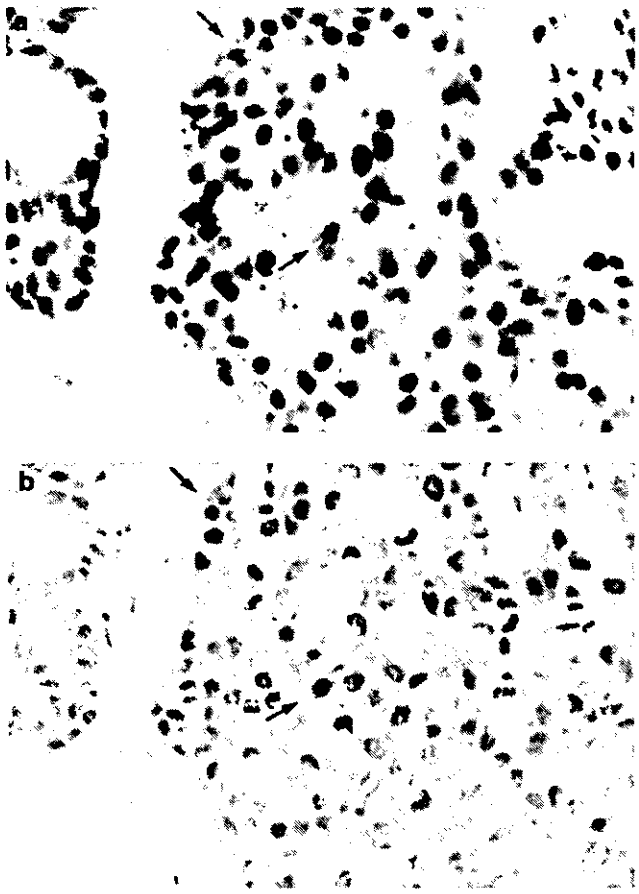

Figure 3 Immunohistochemistry for ER α and β in adjacent sections of breast cancer. (**a**) ER α was detected in the nuclei of cancer cells. (**b**) ER β was detected in the nuclei of cancer cells. Arrows = positive cells. Magnification, × 100.

ER β-negative, and 25 cases were both ER α- and β-positive. In both ER α- and β-positive cases, the distribution of ER α and ER β largely coincided (Figure 3a and b).

As shown in Table 1, all of 19 KGF-positive cases were ER α-positive, while all of 13 ER α-negative cases were KGF-negative ($P<0.0001$). On the other hand, 18 of 19 KGF-positive cases were ER β-positive, and five of six (83%) ER β-negative cases were KGF-negative. Eighteen of 19 (95%) KGF-positive cases were positive for both ER α and β ($P<0.0001$). To assess the direct relationship between KGF-positive cells and ER-positive cells, we performed double-staining for KGF and ERs. As shown in Figure 4a and b, colocalization of ER α or β and KGF in cancer cells was found, respectively. No significant correlation was found between ER expression and KGFR expression.

Correlation between KGF and/or KGFR Expression and TUNEL Index

TUNEL staining was performed to evaluate the correlation between KGF and/or KGFR expression and the frequency of apoptosis. As shown in Figure 5, the percentage of TUNEL-positive cells of both KGF- and KGFR-positive cases was 1.0±0.9%, which was significantly lower than that of other combinations such as both KGF- and KGFR-negative (3.8±2.4%, $P<0.05$), KGF-negative, but

Table 1 Correlation between KGF expression and ER expression

		KGF expression		*P-value*
		−	+	
ER α expression	−	13	0	
	+	10	19	<0.0001
ER β expression	−	5	1	
	+	18	18	n.s.
Coexpression of ER α and β	−	16	1	
	+	7	18	<0.0001

Correlation between KGF expression and ER α expression, ER β expression, or coexpression of ER α and β was examined by χ^2 analysis, respectively. A *P*-value less than 0.05 denoted the presence of a statistically significant correlation.

Figure 4 Double-staining for ERs and KGF in breast cancer tissue. (**a**) Double-staining for ER α (blue) and KGF (brown). (**b**) Double-staining for ER β (blue) and KGF (brown). ER α (**a**) and β (**b**) was detected in the nuclei of cancer cells, and KGF (**a**, **b**) was detected in the cytoplasm of cancer cells. Colocalization of ER α and KGF (**a**) and colocalization of ER β and KGF (**b**) in cancer cells was observed (arrows). Magnification, × 200.

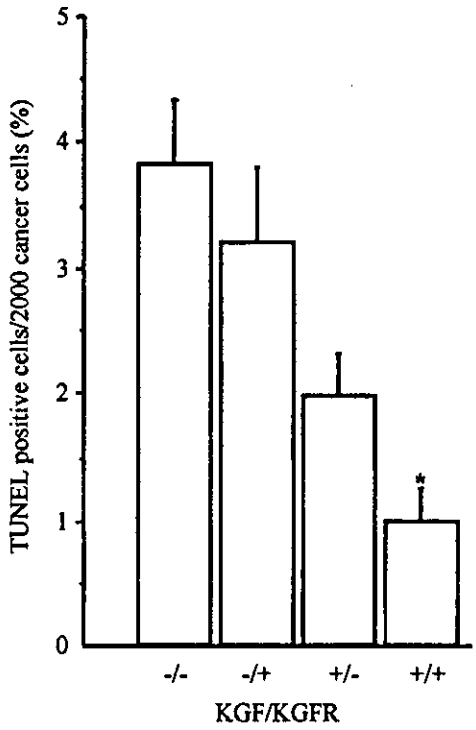

Figure 5 Correlation between TUNEL index and expression of KGF and KGFR in breast cancer tissues. Data are mean value of TUNEL index±s.d. *$P<0.05$.

KGFR-positive (3.2±2.2%, $P<0.05$), KGF-positive, but KGFR-negative (2.0±0.8%, $P<0.05$).

Comparison between KGF and/or KGFR Expression and Cell Proliferation

Ki-67 immunostaining was performed to evaluate the correlation between KGF and/or KGFR expression and the proliferative activity. The Ki-67 LI was 14.8±3.0% for both KGF- and KGFR-negative cases, 15.3±8.7% for KGF-negative but KGFR-positive cases, 12.1±4.3% for KGF-positive but KGFR-negative cases, and 11.3±6.0% for both KGF- and KGFR-positive cases. No correlation was found between the expression of KGF and/or KGFR and Ki-67 LI.

Relationship between ER α and KGF Expression in Breast Cancer Cell Lines

To assess whether KGF expression is associated with ER α expression, ER α-positive and negative human breast cancer cell lines were incubated in the presence or absence of 10 nM 17β-estradiol, and then KGF expression was examined by immunohistochemistry (Figure 6). In ER α-negative SK-BR-3 (Figure 6a and b) and MDA-MB-231 (data not shown) cells, KGF was not detected irrespective of the presence of 17β-estradiol. On the other hand, in ER α-positive MCF7 (Figure 6c and d) and ZR-75-1 (data not shown) cells, KGF was detected similarly in both conditions of 17β-estradiol.

Effect of KGF upon the Induction of Apoptosis in Breast Cancer Cell Lines Treated with Anticancer Drugs

As we confirmed the expression of KGFR protein by immunohistochemistry in MCF7 cells (data not shown), in which the expression of KGFR mRNA was reported,[41,42] we conducted *in vitro* experiments to investigate the effect of KGF upon cell kinetics of MCF7 cells. When we counted the cell number in the presence or absence of 10 ng/ml KGF, no changes in the growth were observed (data not shown). However, when the cells were treated with 500 μg/ml cyclophosphamide or 25 μg/ml 5-fluorouracil in the presence or absence of 10 ng/ml KGF and the number of cells with nuclear fragmentation was counted after Hoechst 33342 staining, the frequency of cells with fragmented nuclei was dramatically decreased in the presence of KGF; 64 and 57% inhibition of the nuclear fragmentation were found in the case of cyclophosphamide and 5-fluorouracil, respectively, as shown in Figure 7.

Discussion

In the present study, we first investigated the expression of KGF and KGFR in human breast cancers at the levels of mRNA and protein, by means of *in situ* hybridization and immunohistochemistry, respectively. We then attempted to correlate the expression of these molecules with various parameters such as ER α and β, Ki-67 LI, and TUNEL index. Consequently, we detected the expression of KGF in breast cancer cells as well as stromal cells, while KGFR was expressed exclusively in the cancer cells.

KGF is considered to be expressed exclusively in stromal cells, and not epithelial cells.[14,15] Indeed, no expression of KGF was detected in normal mammary epithelial cells. In the present study, however, we found for the first time that breast cancer cells expressed KGF in 45% of cases. Since breast cancer cells expressed KGFR in more than 50% of patients, we could assume the formation of autocrine and/or paracrine loops of KGF and KGFR within the cancer tissues. KGF was also detected in ovarian cancer cells, and a possible autocrine action of KGF and KGFR has been implicated in ovarian cancer development.[43] Therefore, the expression of KGF in epithelial cells may not be so unlikely, especially in malignancy.

KGF has been also recognized as a steroid hormone-dependent growth factor in various organs; in rat prostate gland, the expression of KGF mRNA is regulated by androgen,[17] and in monkey uterus, KGF mRNA and protein expression

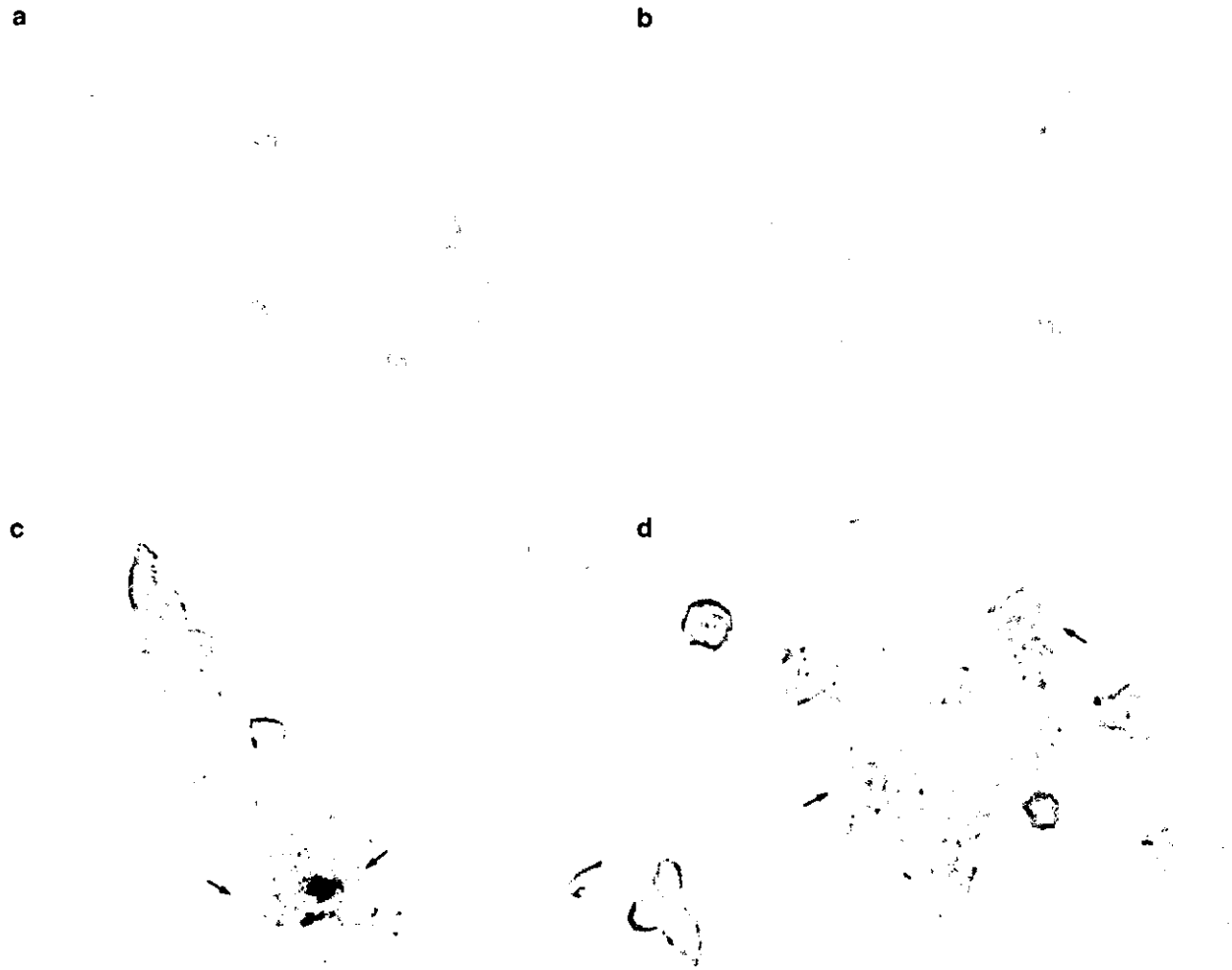

Figure 6 Immunohistochemistry for KGF in human breast cancer cell lines. (**a** and **b**) ER-negative SK-BR-3 incubated in the absence (**a**) or presence (**b**) of 10 nM 17β-estradiol. KGF was negative in both situations. Nulcei were stained with methyl green. (**c** and **d**) Double staining for ER α and KGF in ER-positive MCF7 incubated in the absence (**c**) or presence (**d**) of 10 nM 17β-estradiol. ER α (nuclei, blue) and KGF (cytoplasm, brown) were colocalized in both situations. Arrows = positive cells. Magnification, × 200.

appears to be dependent upon progesterone.[18] Estrogen-dependent elevation of KGF mRNA expression was reported in isolated stromal cells from human breast cancer *in vitro*[20] and in mouse mammary gland *in vivo*.[44] In the present study, KGF expression was tightly associated with ER α expression in surgical specimens of human breast cancer tissues, and KGF was expressed only in ER α-positive human breast cancer cell lines, MCF7 and ZR-75-1. Although unexpectedly, the expression of KGF in these cells was not affected significantly by the presence or absence of estrogen, ER α-dependent regulation of KGF expression may be in a ligand-independent manner. Indeed, estrogen-independent activation of ER by growth factors such as EGF[45] and IGF-1[46] and by the elevation of cAMP[45,46] was already known. Considering that promoter of KGF gene harbors semi-palindromic consensus sequences of the estrogen responsive element,[47] our present study showing coexpression of KGF and ER α in human breast cancer cells provides further evidence of the ER α-dependent regulation of KGF expression.

In the present study, the coexpression of KGF and KGFR in breast cancer tissue was significantly correlated with a lower frequency of TUNEL-positive cells. Moreover, KGF inhibited the induction of apoptosis by anticancer drugs in MCF7 cells *in vitro*. These results seem to indicate antiapoptotic effect of KGF in breast cancer cells. Antiapoptotic effect of KGF was previously reported in human keratinocytes,[22] human prostate cancer cells,[21] and intestinal epithelium of total parenteral nutrition model mouse.[23] In human prostate cancer cells[21] and mouse intestinal epithelium,[23] Bcl-2 is implicated in antiapoptotic effect of KGF. In human breast cancer, Bcl-2 is suggested to inhibit apoptosis, and lower frequency of apoptosis is reported to be a better prognosis marker.[48,49] In this context, KGF might inhibit apoptosis through the elevation of Bcl-2 level in human breast cancer, and coexpression of KGF and KGFR could be correlated with a better